



New STEP-NC-compliant system to automate process planning for the turning process

Abdelilah Elmesbahi¹ · Irene Buj-Corral² · Jihad El Mesbahi¹ · Oussama Bensaid¹

Received: 12 March 2023 / Accepted: 21 June 2023 / Published online: 7 August 2023
© The Author(s), under exclusive licence to Springer-Verlag London Ltd., part of Springer Nature 2023

Abstract

STEP-NC is a smart standard, developed by the International Organization for Standardization (ISO) as a substitute for the ISO 6983 G-code, because the language of the G-Code, normally used for computer numerical control (CNC), is qualified as being unable to link the CAD/CAM/CNC digital chain and meet the needs of modern intelligent manufacturing in terms of tractability, interoperability, flexibility, adaptability, and extensibility. The purpose of this work is to implement the new STEP-NC standard in a computer-aided process planning (CAPP) turning process to overcome the shortcomings of ISO 6893 G-code and enable the process to meet the demands of modern manufacturing. Therefore, the first objective of this paper is to design and implement a CAPP for the turning process, designated as CAPP-Turn, to ensure machining of rotational parts within this modern vision. However, to achieve the CAPP-Turn system, it is necessary to build a robust automatic manufacturing feature recognition (AMFR) module to establish full communication between the first two links of the digital chain, the design CAD and manufacturing CAM, by using a hybrid graph-rules method. The second objective of this work is to elaborate a new consistent-fast algorithm that allows one to extract the machining turning entities for parts with the most efficiency and complex geometry. It then becomes necessary to introduce the main machining entities defined within the framework of this standard and to explain the different parameters that are necessary for the unambiguous definition of these entities whether of a geometric, topological, or other nature. In fact, most of the AMFR systems presented in the literature are restricted to the external turning process and cannot handle parts with complex geometry and interacting features. Moreover, the frontal turning features are largely neglected in most of these systems, despite their importance for fulfilling certain functions in mechanical systems. This article first details the global architecture of the CAPP-Turn and clearly describes the interaction between the CAD part and STEP-NC output file. It then explains the model of the AMFR system, which encompasses (i) a parser module that translates geometric and topological data from a STEP AP203 CAD file into Python entity class objects; (ii) an AMFR that analyzes the objects created and applies predefined rules to construct all possible turning machining; and (iii) a module capable of distinguishing external features from internal, frontal features from axial, and handling interacting features from the simple features. After these steps, the AMFR provides all suitable sequencings for part machining. Finally, to demonstrate the potential advantages and power of the proposed AMFR, a selected part is chosen for testing. The result shows that the AMFR performs well in recognizing all types of features regardless of their type: internal or external, axial or frontal, simple or interacting.

Keywords Turning process · CAPP · STEP-NC · CAD/CAM/CNC · Automatic manufacturing feature recognition · Interacting features · Frontal turning features

✉ Jihad El Mesbahi
Jihad.elmesbahi@gmail.com

Abdelilah Elmesbahi
elmesbahi_abdelilah@hotmail.com

Irene Buj-Corral
Irene.buj@upc.edu

Oussama Bensaid
oussamaabensaid@gmail.com

¹ ISEEC, Industrial Systems Engineering and Energy Conversion Research Team, Faculty of Sciences and Techniques, Abdelmalek Essaâdi University, Tangier, Morocco

² ETSEIB, Universitat Politècnica de Catalunya, Mechanical Engineering, Barcelona, Spain

1 Introduction

The CAD/CAM/CNC chain was principally designed to facilitate the successful manufacture of a part and obtain its physical model using a digital CAD file and adhering to different specifications. This chain classically consists of an open-tree of three links. The first is the computer-aided design (CAD), in which the engineering office (designer) creates the geometric model of the mechanical part and attributes to it different specifications and tolerances to ensure its functionality once it is placed in a mechanical system. After this step, the method office creates a workplan to define the sequence of machining operations, machines and cutting tools, clamping, and cutting condition parameters. In the third step, to guarantee numerical control (NC) of the fabrication, a digital machine programmer creates, manually or by using CAM software, the classical G-code, which is the oldest international standard language available under the reference RS-274D (ISO 6983). In modern industry, manufacturers must confront new challenges beyond the study of the feasibility of fabricating a product, because they must prepare it for competition which will arise within the context of Industry 4.0. Then, they must agree to adopt a novel, intelligent numerical chain that can provide fully optimized management and manufacturing of the product, by sweeping and integrating its entire life cycle. From this perspective, the current G-code, developed in the 1960s for NC, is not able to perform this key task, because it breaks the bidirectional communication between links of the numerical chain and limits the tractability, flexibility, and interoperability of manufacturing systems. Thus, over the last decade, many efforts have been devoted to merging the standard for the exchange of product model data (STEP) and STEP-NC into their computer-aided process planning (CAPP) in order to benefit from these advantages. This standard has touched all manufacturing processes, mainly those used in machining. However, in the following, we present only the state of the art related to the manufacturing automatic recognition systems that have specifically used STEP and STEP-NC as processing formats. At the same time, we review the performance and a few points of weakness of the systems mentioned.

Sivakumar and Dhanalakshmi [1] developed a system using a simplified and generalized method for cylindrical parts which allows the extraction of information regarding machining characteristics from STEP files. The extracted data are used to generate NC codes according to the type of controller. The method was validated by machining the cylindrical parts generated by the codes and inspecting the part using a three-dimensional coordinate measuring machine (CMM). However, the processing of cylindrical

groove entities is not indicated in this work, and the programming of the NC machine is apparently carried out via the classic G-code and not STEP-NC. The software developed by Malleswaria et al. [2] ensures the recognition of the various character strings in the STEP file and allows their interpretation in terms of turning machining entity. Recognition is reinforced by technical rules. The recognition module proposed by the authors is able to identify cylinders and axis holes located in a plane perpendicular to the axis of revolution (asymmetric parts). This method is based on a character string process requiring considerable processing and does not benefit from the potential data structuring offered by the objects already present in the STEP file. The thesis project [3] “Design by Entities for parts of revolution based on STEP” aims at extracting machining entities from STEP AP224 for parts of revolution. The STEP AP224-generated entities are used as basic entities to draw the part. The technique enables the definition of entities, their classifications, the addition of attributes and geometric constraints. The object-oriented design used in the development of modeler entities ensures improved performance and reusability of these entities. The STEP-XML file of created data can be used in the CAPP/CAM chain without the use of a complex recognition system. Although this system makes it possible to generate STEP AP224 entities, the design-by-entity approach considerably limits system operation. The feature library remains incomplete due to the lack of repetitive, complex machining characteristics for exterior turning and other characteristics for reaming. Also, the interacting entities are not taken into consideration within the framework of this work. In the end, this work, restricted to the recognition phase, does not make it possible to specify the method, the format and the type of the code used to transmit the entities generated to the NC machine. Similarly, Sharma and Gao [4] designed a new-generation process planning system based on the machining characteristics technique and using the international STEP AP224 protocol. The system does not require any intervention from the user for the generation of machining schedules and supporting documents. It consists of decision logic stored in an external database, which makes it generic and compatible with any manufacturing process. Likewise, it is equipped with a feature model editor (FME) used as a design tool by entities, with simple components. The same criticisms as before can be formulated with regard to this system. The generated data are then used in shop floor applications, such as machining schedules, production optimization, machining simulation and manufacturing control, that require access to integrated data from product manufacturing. However, this third-generation system still needs to be improved, and collaboration with the machine manufacturer is thus required. Unlike other research which has generated G&M codes or other CNC machine-specific programs from STEP-NC to bypass CNC machine tool information

[5–7], Shin et al. [8] proposed an inverse approach which allows the extraction of manufacturing information from the G&M code to generate the STEP-NC program in the case of a turning process. This approach remains very difficult due to the low level or absence of information on the production range in the G&M code. However, according to Suh and Lee [9], this manufacturing STEP roadmap is an essential step to replace G&M codes with STEP-NC for the interoperable manufacturing era. The process planning system (PPS) proposed in [10] presents three interesting features: (i) STEP-NC data can be used to generate standardized data for generic process planning and definition of trajectories of the process tool for turning operations; (ii) with the incorporation of the surface roughness modulus, PPS can be integrated with STEP-NC data to generate production routings with prediction of surface quality; and (iii) this research investigated the timeliness of the optimization process using a manufacturing knowledge base contained in STEP-NC. The authors specify that supplying STEP-NC with sufficient information makes it possible to optimize the manufacturing variables and to move towards intelligent manufacturing. Stimulated by industrial needs for simultaneous engineering, Yusof and Case [11] designed a CAD/CAPP/CAM system called SCSTO (STEP-NC-Compliant System for Turning Operations) based on STEP ISO14649 for the manufacture of asymmetric parts over-milling CNC turning. This system aims to model information in the field of mechanical manufacturing by addressing the problem of capturing and representing data related to resources and processes. The interaction between the different types of models provides a description of the products, the method and the resources that will be needed to ensure their manufacture. The STEP-NC generator code generates a Part 21 file based on the machining characteristics to make iterative the generation of automatic ranges during the entity extraction phase. The designed system adopts a structured methodology for its planning and object-oriented methods for its implementation. Case studies were tested to show the new coding approach (STEP-NC) used can intelligently replace the G-code currently in use while providing some benefits such as elimination of the post-processor. However, the authors specify that there is still some effort to be made to revolutionize certain axes in the system: combination of Parts 11 and 12 for turning/milling operations. The TERMINAL STEP-NC software [12] presented can take into account parts with a geometry composed of cylindrical and conical surfaces and can also be extended to other types of surfaces and to new functionalities. This platform makes it possible to build a complete database of machining and its related information. By using STEP-NC as a potential tool, the authors were able to reduce the time required for programming the CNC by around 35%, decrease the number of

drawing files transmitted from design to manufacturing by 75% and achieve savings of 50% on time necessary for the machining of parts on the CNC machine tools for work in small and medium series. The authors qualify STEP-NC as bringing potential future development opportunities for mass manufacturing. In Suh et al. [13], the authors present a turning system called Turn STEP. The data model used was developed by the STEP-NC research team of the POSTECH National Research Laboratory of South Korea in collaboration with ISW University Stuttgart, Germany, and formalized as ISO 14649 Part 12 and Part 121. The architecture behind Turn STEP is based on various considerations of a transparent and intelligent CAD/CAM/CNC chain from the future e-manufacturing paradigm. Although Turn STEP was in the prototype stage, the validity of its data model and the efficiency of its architecture have been proven, and it has been shown that CNC systems based on STEP-NC have enormous potential and power compared to conventional CNC systems based on the old ISO 6983 standard used for over 50 years. The two German institutes, Institute for Machine Tool Control Engineering Manufacturing Units (ISW) in Stuttgart and the Laboratory for Machine Tools and Production Engineering (WZL, RWTH) in Aix, played an important role in the European STEP-NC project. Their research contribution was focused on STEP-compliant development and implementation. The sophisticated Turn STEP turning system is a CAPP for connecting CAD and CAM. It first reads geometric data from a STEP AP-203 Part 21 file, then performs routing planning tasks such as feature recognition and operation sequencing to generate a physical STEP-NC file. [14]. However, this system cannot be used on any other controller other than the Siemen 840. Hardwick [15] developed the third generation of the STEP system which combines data from existing systems to generate new data. This system has been successfully tested on the milling process and on defined turning applications. The first generation of the system uses the Express model as an input and Java as a programming tool, while the second generation is improved by adding tools to visualize and validate the data defined first by the application protocols of STEP. This generation can read, write and exchange the data of the two protocols AP203 and AP214. Finally, the third generation proposed makes it possible to receive various XAO sources. This system is connected to a workshop via the standard STEP AP-238 protocol from data produced. The CAD data and tool trajectories and the manufacturing data from the CAM module are then used to combine STEP and Geometric Dimensioning and Tolerancing (GD&T) parameters within a direct interface or legacy format.

Table 1 cites the research carried out on STEP-NC with an emphasis on turning and turning/milling processes [16].

Table 1 Research work using STEP-NC carried out on the turning and turning/milling process

Ref.	Process			Standards		Data storage	
	Mill	Turn.	Other	AP238	ISO 14649	XML	TEXT
Rosso et al. [18]	☒				☒		☒
Xu and al. [19]	☒				☒		☒
Xu [20]	☒				☒		☒
Chen et al. [21]	☒			☒			☒
Suh et al. [22]	☒				☒		☒
Choi et al. [23]	☒				☒		
Heusinger et al. [24]	☒				☒		☒
Yusfo 2006 [25]	☒				☒		☒
Shin et al. [26]	☒				☒		☒

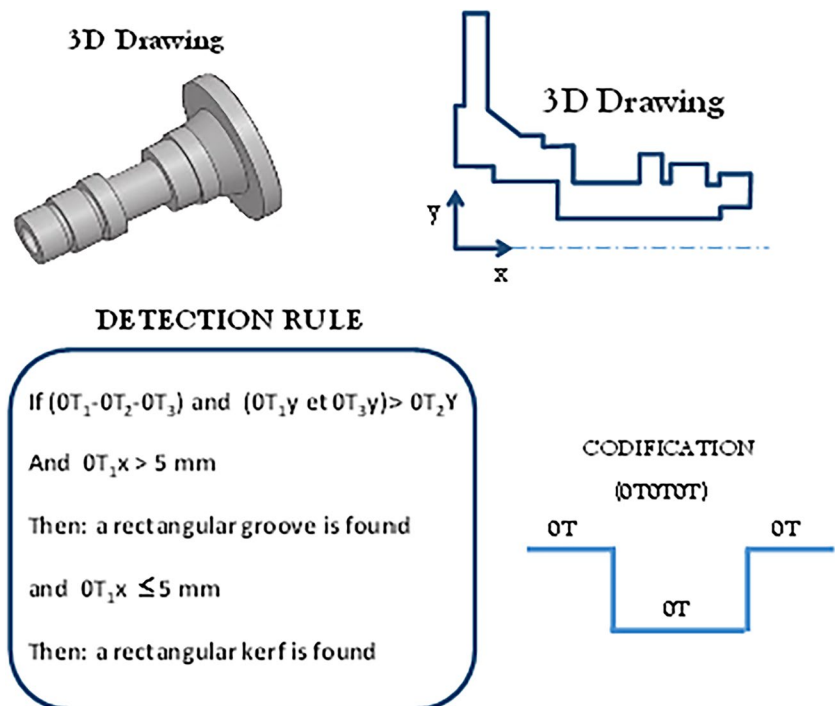
2 Review of related works

The process of manufacturing feature recognition (MFR) is the most complex module of any CAPP in the machining sequence. The algorithms developed for MFR for turning process are diverse in terms of techniques adopted (attribute adjacency graph, volume decomposition, hybrid

approaches, syntactic pattern recognition, etc.), mathematical model developed, and input CAD used. In the algorithm of machining entities extraction [26], the input CAD model is a three-dimensional (3D) drawing saved in a neutral STEP AP 203 file simplified into two dimensions. The recognition method is based on reasoning rules applied on the two-dimensional (2D) drawing. The proposed system succeeds in extracting the data and characteristics of the part to be turned. Designed to be self-sustaining, the algorithm is programmed in Visual Basic 2008 connected to the EWD raw module. By studying the information contained in the STEP AP203 file, rules for constructing 2D entities from 3D entities are established: for example, in STEP, a simple cylinder consists of two planar and two cylindrical surfaces. For the 2D representation of the cylinder, 12 states are needed. The cylindrical faces contain four curves with line segments and four curves with circular segments, and the two planar faces contain four curves with circular segments. By intelligent selection of the desired lines, the 2D drawing of the cylinder can be represented in two dimensions. In turning entities, there are three main body types: cylindrical, conical and toroidal. The inner entities, in STEP AP203, are often coded by the letter F, and outer entities by the letter T. Horizontal lines are coded by 0, inclined by 1, vertical by 2 and curvilinear by 3. For example, the outer circular groove is coded by 0T0T0T. The principle of the method is given by Fig. 1.

Qin and Li [27] provided an intelligent method of machining in turning based on the recognition of geometric characteristics. Their algorithm is designed to recognize

Fig. 1 Principle of the method for extracting turning entities [26]



the planar faces, turning contours (cone, trunk and cylinder) and grooves by defining a point of view, a direction and the cylindrical coordinates for true loops and false loops in projection. By creating functions connecting all the loops, the algorithm determines the regions to be machined in turning. According to the authors, the study solves the machining ability problem during the design stage and reduces costs and saves production time. This method of feature recognition is described by Fig. 2 as follows: A point P_i of the part is defined by the cylindrical coordinates $P(r_i, \theta, Z_i)$. The approach consists in identifying the largest contour of each real loop l_i , its radius r_i , and its length (ΔZ) and the function $\theta(r, z) = f(r, Z)$ connecting the two variables r and Z . If Δr is zero, then the extent of the real loop is a cylindrical part; if ΔZ is equal to zero and Δr is not zero, then it is about a plane face delimited by two true loops. Otherwise, it is a part to be machined in turning, for example, a cone or a trunk cone. The regions between the part outside each cylinder of the part (conical or trunk-conical) and the inside of the visibility space, defined by the radius R , must be machined.

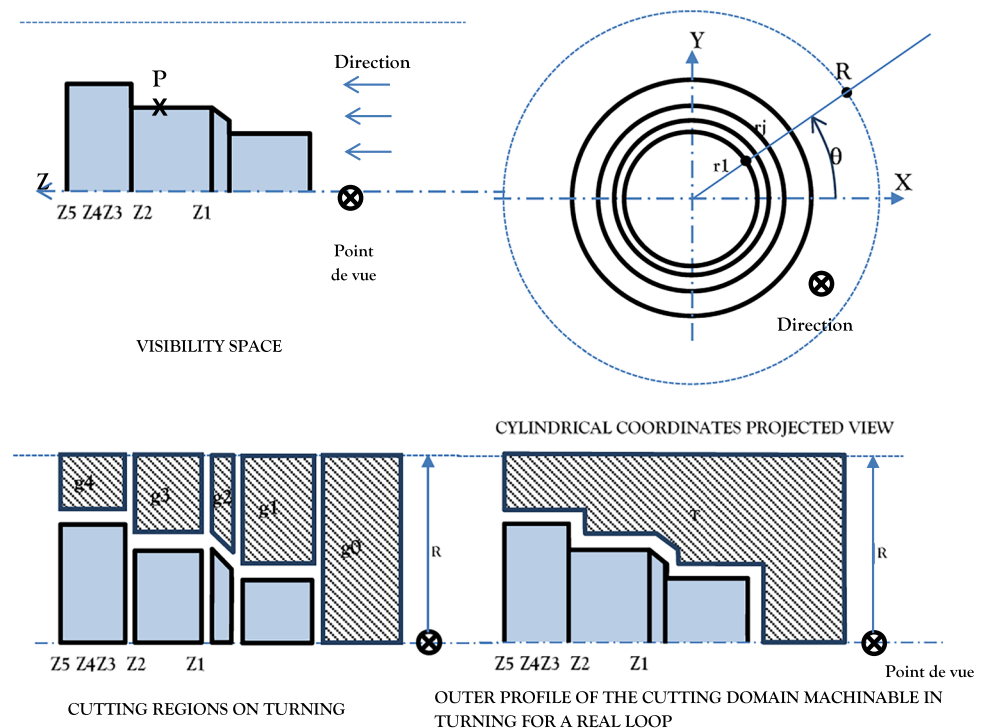
Chung and Peng [28] present an FAR based on the CAD Drawing Interchange Format (DXF). The design of the part is represented by geometric entities such as lines, curves and surfaces. From a DXF data file, the recognition of machining entities begins by obtaining the simple geometric elements used for its construction. Figure 3a briefly represents the steps followed for the conversion of the geometric information contained in the DXF format into geometric entities as defined by

this method: a line entity is converted from DXF format (AcDbLine or AcDbPolyline) and stored in a defined entity format (line_type, Point1, Point2). Line_type defines a straight line or a line tangential to a circle. In particular, if a line feature of a DXF file includes the number 42, it will need circular interpolation in the next line, because the DXF format does not provide information about the circular connection of the two lines. The circular entity interpolated here is also stored in a circular entity format defined by Circular_direction, Center_point, Start_angle, End_angle and Radius.

Once the geometric entities are obtained and stored, the next procedure converts these elements into machining entities using the decision-making diagrams. Three types of decision-making diagrams are developed to handle three simple geometric features of cylinder, cone and dome, to which the thread wrapping entity has added.

The extraction of the entity is explained with reference to Fig. 3b: if the entity of the second layer is of the same linear type as that of the first layer, it may be a recess L-void (hole flat bottom) or an E-thread threaded cylinder; it depends on the type of the following entity. Based on these rules, a machining entity can be formed from the geometric elements obtained. In particular, an object-oriented manufacturing feature (OOMF) machining entity strategy based on object-oriented programming (OOP) is introduced to efficiently store and manipulate the defined machining entity. Figure 4 gives an overview of the hierarchical diagram of the OOMF classes.

Fig. 2 Method of recognition of the characteristics of machining in turning proposed by Qin and Li [27]



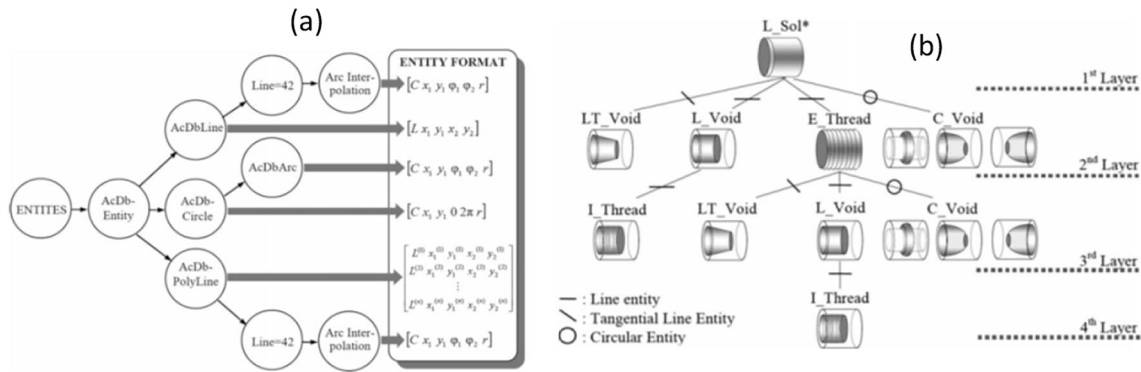
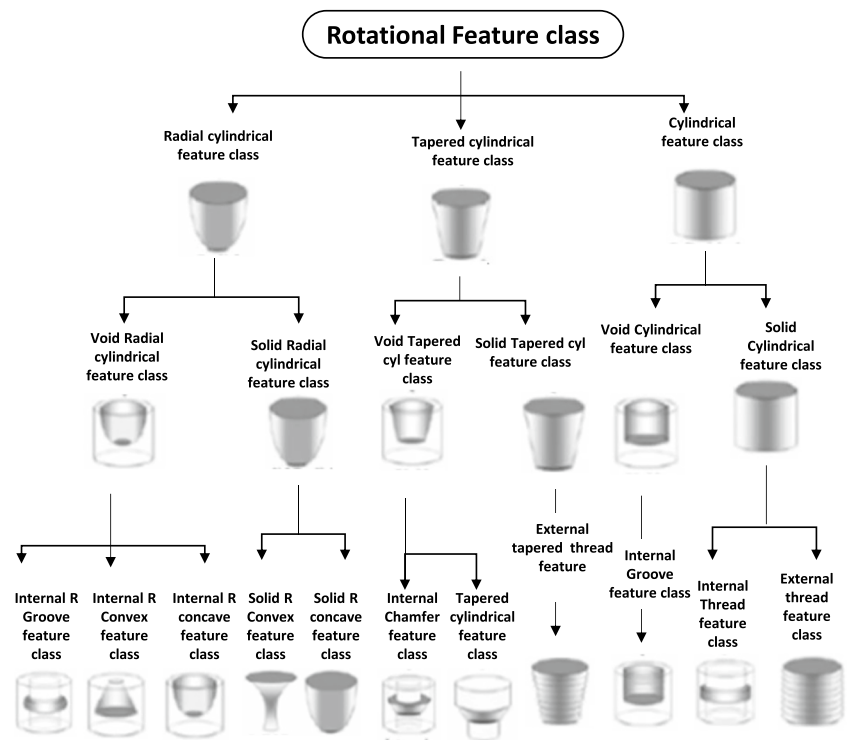


Fig. 3 a Steps for converting geometric entities from information represented in the DXF file and (b) decision diagram developed for the definition of the machining entity from the geometric elements obtained

Fig. 4 Hierarchical diagram of the OOMF classes



The Automatic Entity Recognition System [29] comprises three modules: (1) a CAD module for part drawing using Mechanical Desktop; (2) a feature extraction module based on a new low-level algorithm (point coordinates, vector direction and its modulus) using the STEP profile (ISO 10303, Part 21) of the part generated from the previous module; and (3) an automatic entity recognition module, which is a knowledge-based subsystem. In this module, an automatic feature recognition (AFR) algorithm called sweeping primitive rule (SPR) is built based on three recognition techniques (Fig. 5): (a) syntactic model; (b) scanning operation; and (c) logical rules. The SPR algorithm is intended to increase the flexibility of recognizing different types of simple features

(cylindrical, grooves and shoulders), in addition to new features of compound types for symmetrical rotational parts.

The identification method can be described as follows: After extracting all the Cartesian points from the part's STEP file, rules are used to define the line entities in Fig. 5b. A second syntactic form encoding is ensured to convert the entities obtained into new oriented lines (line a, b, c, d, e, f and g), as shown in Fig. 5c and e. Then rules are applied to ensure the automated recognition of entities, as in Fig. 5d.

The study presented by Yildiz [30] describes an AFR system equipped with a CNC code generator (automatic feature recognition and CNC code generation, AFR/ACCG) designed for revolution parts. This system has been

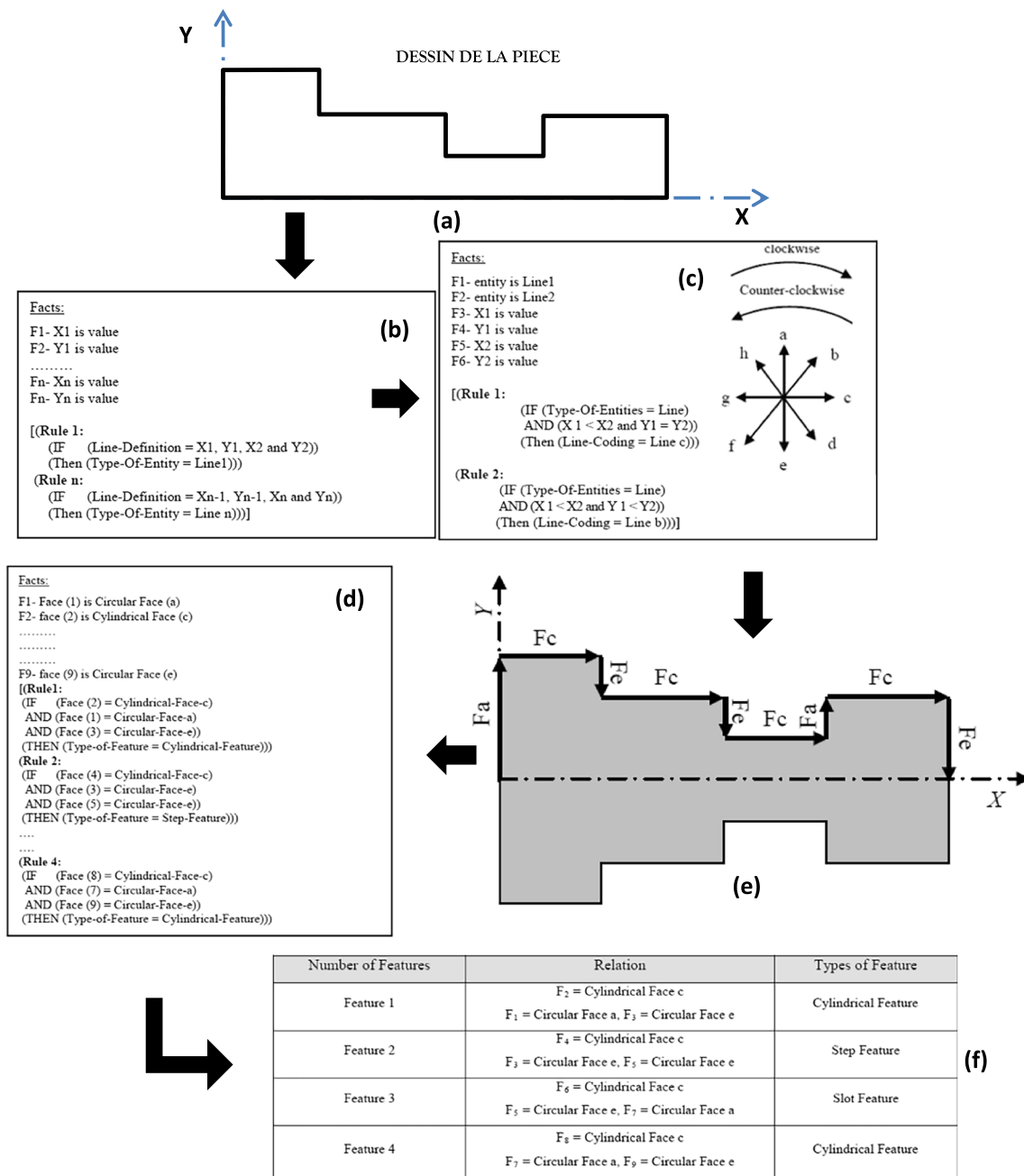


Fig. 5 Principle of the FAR algorithm proposed by Hussein Salem Ketan [29]

programmed using Delphi language. CAD data input to the system is done in DXF available in almost all CAD software. The CNC G-code program of the workpiece is generated automatically, as is the case with entities. By generating the toolpaths and using the part geometry, sample parts were machined with precision. The system can be enriched by new machining entities by making the definitions necessary for their addition. The step of recognizing machining entities begins after importing the DXF format where the drawing entities are identified and are defined in the system. At this

point, the coordinates of the two starting and ending points of the arcs, which cannot be accessed by the DXF, are found using trigonometric equations, and all the coordinates found are classified from right to left and from bottom to top.

Following the authors, this classification provides a precise feasibility of the sequencing process to be followed in the next steps. As it is possible to have a drawing positioned anywhere in the CAD environment, according to the Cartesian coordinate system, the latter are then modified to have a quadrant II ($x < 0, y > 0$) of the coordinate system, because

the toolpaths are constructed, generally, with respect to the face of the cylinder to be machined. After this phase, all the coordinates of the geometric entities are sequenced according to their starting points and positioned relative to the origin. Thus, all the basic geometric entities (lines and arcs) which are generated are represented separately for all the turning operations as illustrated in Fig. 6a and b. The system classifies machining characteristics into inner and outer entities based on their machining attributes. These two feature classes are also further subdivided into subgroups such as long turning, grooving, threading, and reaming. Finally, the profile of the work piece is produced by the program. The direction and sequence of recognized machining entities for a test part is shown in Fig. 7.

3 Methodology of CAPP-Turn elaboration

3.1 Data CAD input for MFR of CAPP-Turn

The key step to begin an automatic feature extraction is the extraction of geometric and topological information from the STEP CAD. For this purpose, we use STEP-AP203 standard CAD as the entry of the system. A detailed description of this standard can be found in [31].

Figure 8 gives the hierarchical structure of the entities defined in STEPAP203 based on the CAD modeling of revolution parts. The highest level in this hierarchy is the CLOSEDHELL entity that is used to define the solid part. This element is formed by a set of connected advanced faces (ADVANCED_FACES). At each advanced face one type of geometrical surface is bounded (FACEBOUND) that can be planar, cylindrical, conical, spherical, etc., and one type (FACEOUTERBOUN) (topological definition) that specifies the set of oriented edges/borders of the surface. The description of the part continues until it reaches the vertex/point which is the lowest level of the hierarchy.

The basic idea for designing the machining entity recognition system for the turning process is to cover the majority of the operations of this manufacturing process. Turning operations are classified into exterior and interior turning (reaming). In the case of exterior turning, a distinction is made between turning cylinders and cones, dressing, producing shoulders (turning combined with dressing), external grooving, making slits, taking off, profiling and some operations. Dressing includes threading, chamfering, machining of fillets and knurling (Annex 1: Table five). Internal turning comprises cylindrical and conical bores, internal shoulders, recesses, grooves, internal grooves, and naturally some trim entities such as threading, chamfering and making fillets (Annex 1: Table six). It must be noted that the turning operations have been conventionally defined by referring to the trajectory of the tool with respect to the part, and

thus the stock removal is defined as the operation consisting in machining a cylinder of a certain diameter by displacement of the cutting tool along an axis parallel to the axis of rotation of the part, but our work is based on the machining entity which is a characteristic of the part (geometric, topological, tolerances, etc.) and which will be machined. The difficulty resides, therefore, firstly in the possibility of capturing this entity regardless of the geometry of the part to be turned and secondly to ensure the machining of the detected entity using the recognized machining operations.

To elaborate a new consistent-fast algorithm that allows the extraction of the machining turning entities for parts with the most efficiency and complex geometry, it becomes necessary to introduce the main machining entities defined within the framework of this standard and to explain the different parameters that are necessary for the unambiguous definition of these entities whether of a geometric, topological or other nature, in order to remedy the shortcoming of ISO 6893 G-code to overcome modern manufacturing demands.

Figure 9 gives the EXPRESS G diagram summarizing the main turning machining entities which are defined by the International Standard STEP ISO14649-12. Table 2 gives the various parameters defining these entities.

The turning machining entities defined by the STEP ISO14649-12 standard are, generally, parameterized entities which can represent a set of entities according to the setting of its parameters, as well as the outer diameter entity, defined by its small diameter (diameter_at_placement), its angle (or its large diameter: diameter_taper) and its feature_length height, can represent a cone in the case where the tilt angle is different from zero and a cylinder in the case where this last parameter is zero (or diameter_at_placement = diameter_taper). This entity is described by STEP-NC as follows:

```
ENTITY outer_diameter
SUBTYPE OF (outer_round);
diameter_at_placement: toleranced_length_measure;
feature_length: toleranced_length_measure;
reduced_size: OPTIONAL taper_select;
END_ENTITY;
```

Apart from the geometric and topological parameters, the ISO 14649 standard makes it possible to define a local coordinate system for each entity (Table 2).

This coordinate system is used to locate the position and orientation of the entity in relation to the part to be worked. It should be noted that this location remains a determining factor for the starting positioning of the cutting tool in order to ensure the machining of the feature. In addition, all turning machining entities inherit the feature_placement attribute (defined by Part 10 of ISO 14649) from the parent class Two5D_manufacturing_feature This element specifies

Fig. 6 Methodology of manufacturing feature recognition following [30]

Operation Types of Using Features	Types of Geometric Features		Rules for Feature Recognition	Feature Number
	External	Internal		
Long Turning, Profile Turning Grooving, Threading Drilling Boring			$(y1 = y2)$	1
Facing Out Profile Turning Grooving Drilling Boring			$(x1 = x2)$	2
Profile Turning Grooving Drilling Boring			$(x1 < > x2)$ & $(y1 < > y2)$	3
Profile Turning Grooving Drilling Boring			$(x1 < > x2)$ & $(y1 < > y2)$	3

(a)

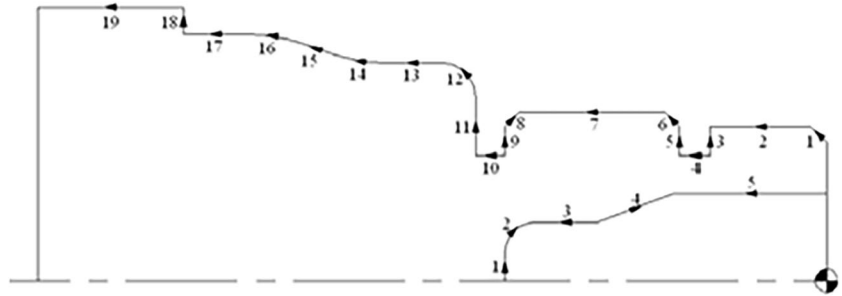
Operation Types of Using Features	Types of Geometric Features		Rules for Feature Recognition	Feature Number
	External	Internal		
Profile Turning Grooving Boring			$(a1 \geq 0)$ & $(a2 \leq 90)$	4
Profile Turning Grooving Boring			$(a1 \geq 180)$ & $(a2 \leq 270)$	5
Profile Turning Grooving Boring			$(a1 \geq 90)$ & $(a2 \leq 180)$	6
Profile Turning Grooving Boring			$(a1 \geq 270)$ & $(a2 \leq 360)$	7
Profile Turning Grooving Boring			$(a1 < 90)$ & $(a2 > 90)$	8
Profile Turning Grooving Boring			$(a1 < 270)$ & $(a2 > 270)$	9

(b)

the current position of the feature relative to the workpiece coordinate system and is defined by translating and/or rotating the origin of the feature's local coordinate system

relative to that of the workpiece. The feature_placement attribute is described, according to ISO 10303–238, by the Axis2_placement_3d class which has three attributes: two

Fig. 7 Direction and sequence of recognized machining entities for an example part [30]



optional attributes (*Axis* and *Ref_direction*), which define the directions of the local *x* and *z* axes of the entity and the third Cartesian_point, materializes a point of coordinates *x*, *y* and *z*, coinciding with the origin of the coordinate system of the entity, and located in relation to the origin of the coordinate system of the part. According to ISO 10303–238, we note that the definition of the class *Axis2_placement_3d* is obviously the same as that of ISO 10303–203. The UML diagram of Fig. 10 gives the class allowing us to completely define the cylinder entity (*outer_diameter*).

3.2 Turning feature graph modeling

The process that we are going to put in place for the recognition system is very simple: (1) To be able to discretize the part into elementary geometric/topological entities of revolution present in STEP AP203 such as planes, cylinders, cones, spheres, and B-splines. The hierarchical structure of the STEP AP203 protocol summarizing the different elementary entities used is shown in Fig. 8. (2) Use rules to build basic entities overriding the definition of turning machining entities. This idea is original in the fact that it allows, on the one hand, optimization by the use of the basic entities just necessary for the construction of all the machining entities because a basic entity can participate for the constitution of several machining entities of different types. On the other hand, this concept makes it possible to represent the outer and inner elementary entities by the same entities before proceeding to the stage of differentiation between them. (3) The weaving of basic entities to obtain the desired turning machining entities. (4) The standardized writing of turning entities formed according to ISO STEP-NC.

To extract all the machining entities, the two approaches, in series and parallel, adopted in this work are the same as that of the CAPP of milling previously developed [31, 32]. Given the nature of axial symmetry characterizing the parts worked in turning, all parts can be seen as a series association of elementary geometric entities connected by circular entities (circles in tipped point), as shown in Fig. 11.

In this model, the surface entity detected will be modeled by a vertex, and the border circles represented by the arcs are the connecting junctions (adjacency) with the two

neighboring entities. Normally, four types of entities can be distinguished in a part according to the position of the entity in the part and also of its type (Fig. 12). In type I, the axis of revolution of the entity is completely defined by the two centers of the boundary circles. For type II, its axis is identified by the vertex of the center of the surface and the center of the circle shared with the following entity. Types III and IV are characterized by the flat surface nature defining the surface of the entity; their axes of revolution are completely characterized by the center of the plane and its normal pointing towards the outside of the material. Thus, graph models of each entity and its correspondents are given by Fig. 12:

3.3 Rules for the identification of manufacturing features

In our approach, an elementary feature *i* is modeled by the following: (1) a numbered vertex *i* representing the surface entity to be extracted; (2) the bounds of the surface which are either circles C_i and C_{i+1} or a vertex V_i and a circle C_i . The circles C_i and C_{i+1} define the junction profiles (adjacency) of the feature *i* with feature in upstream *i*-1 and downstream *i*+1 of this surface. The vertex V_i represents the center of the free surface where there is no connection; (3) the axis of revolution of the entity which is defined either by the two centers C_i and C_{i+1} or V_i and C_{i+1} for the surfaces of revolution, or by the center of the circle and the normal resulting from this center on the material-free side for features with a flat surface.

To check that the part is of revolution type, without the presence of asymmetric elementary features, all axes of symmetry of the elementary detected features must be naturally coincident.

To construct a total isomorphism graph of the part, we start with an arbitrary elementary entity of the part, and we take its axis as the axis *Z* of revolution of the whole part and its end coordinate *Z* minimum as the provisional origin of local reference to be assigned to the part. The model of the final part is constructed by association in series of elementary features by fusion of the common circles of junction. The final graph model of the 3D part is presented in Fig. 11. For the identification of elementary features, the rules are

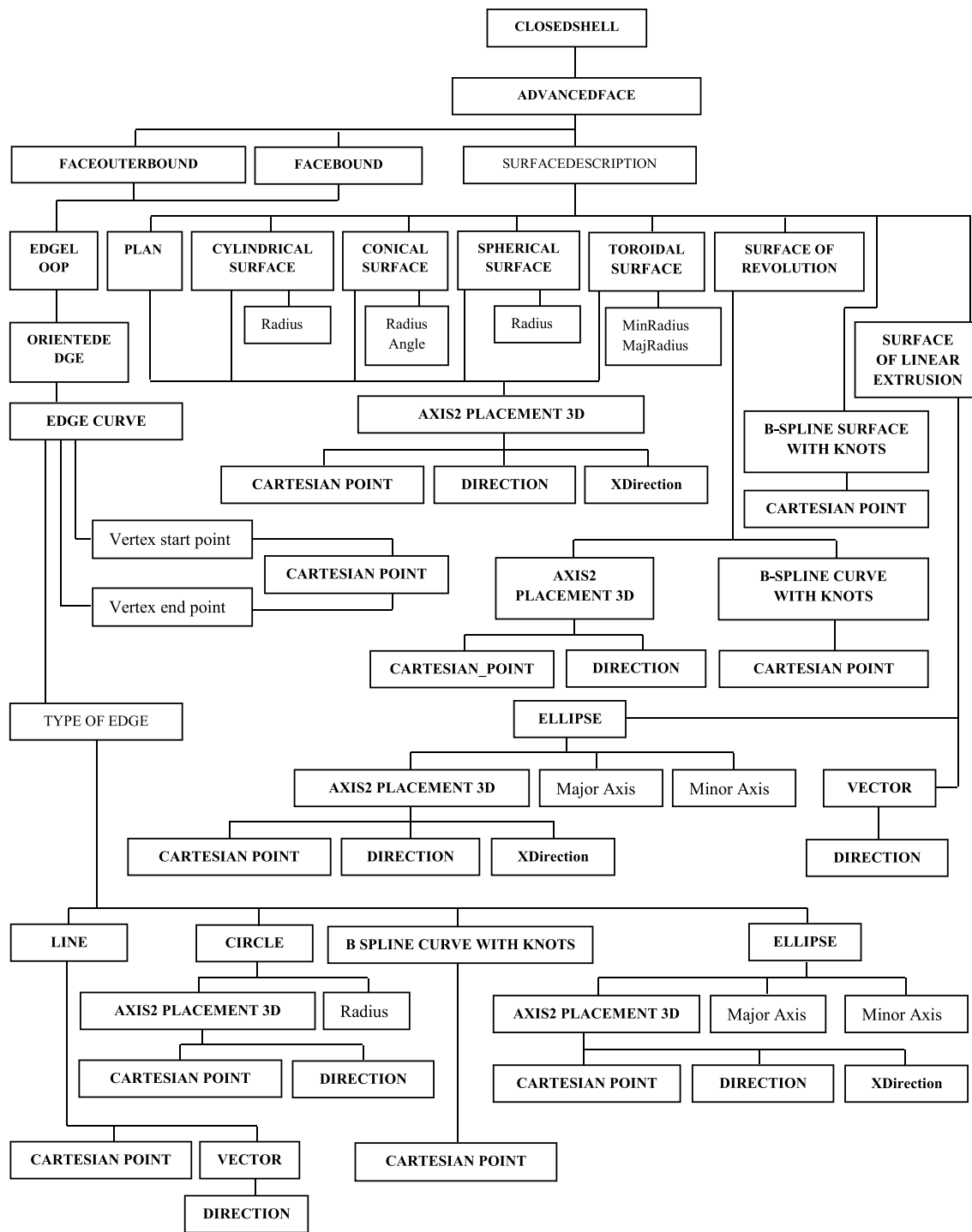


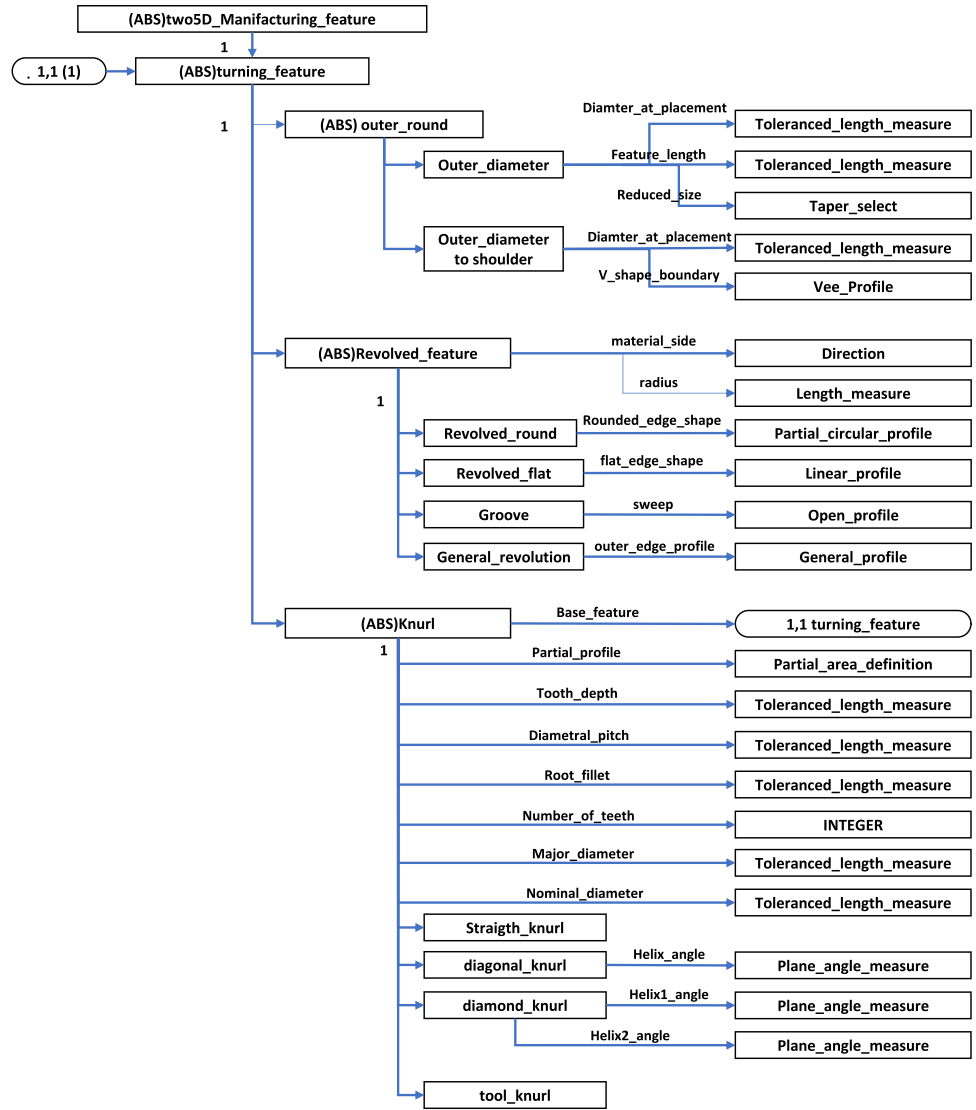
Fig. 8 Hierarchical structure of the entities defined in STEP AP203 [30]

compiled by first using the topology of the part and, if necessary, we add the geometry criterion. This preference is allowed to ensure more degrees of freedom in terms of the dimensional variability of the entity.

The EXPRESS modeling, Python language and the STEPCode library are the main tools used to map

parameters of objects representing manufacturing features obtained by the AFR system to geometric and dimensional attributes of classes representing features of ISO 14649. The established rule for the identification of an elementary cylinder is graphically explained by the flowchart of Fig. 13. The identification of this

Fig. 9 Direction and sequence of recognized machining entities for an example part



element consists of four rules obtained from EXPRESS LANGUAGE AP203:

Rule 1: The STEP CAD file must contain at least two cylindrical surfaces (Cyl 1 and Cyl 2), each delimited by a loop formed by the entities including a circular segment (Arc Cir), linear segment (Line), circular segment (Arc Cir), and a linear segment (Line): Cyl 1 (Arc Cir 1: C11, Line 11: L11, Arc Cir 12: C12 and Line 12: L12) and Cyl 2 (Arc Cir 21: C21, Line 21: L21, Arc Cir 22: C22 and Line 22: L22).

Rule 2: L11 must be the same as L21 or L22.

If L11 is the same as L21, then L12 must be the same as L22; if not, L12 must be the same as L21.

Rule 3: The two pairs of circular edges that share the same vertices must have identical centers.

Rule 4: The two pairs of circular edges which share the same vertices and which have the same centers must be distinct (not confused).

The algorithms used to scan and detect other types of turning features from the STEP AP203 model are summarized in Table 3 and its continuation in Appendix Table Five.

3.4 Consideration of transformation elements and scale

Knowing that a 3D definition drawing of a part may have an offset from the origin of the reference system of the CAD software and any orientation with respect to that system, critically, the drawing of the part can be enlarged or reduced according to the scale of the adopted design. These operations are commonly referred to as affine transformations applied to an object and do not affect the topology

Table 2 Principales Entités d’Usinage de Tournage définies par STEP ISO14649-12

Machining entity defined by STEP	Explanatory diagram	Description
outer_diameter		$0 \leq \text{corner} < \frac{\pi}{2}$
outer_diameter_t o_ shoulder		$0 \leq \text{corner profile} < \pi$ $0 \leq \text{profile radius} \leq +\infty$
revolved_flat		If the stop is vertical, we find the face entity
revolved_flat		In the particular case where the right end of the arc coincides with the axis, we reproduce the end of the sphere
Groove (a) : facial and (b) radial		According to ISO 14649-10, open_profile can be square_u_profile, rounded_u_profile, partial_circular_profile, and general_profile

Table 2 (continued)

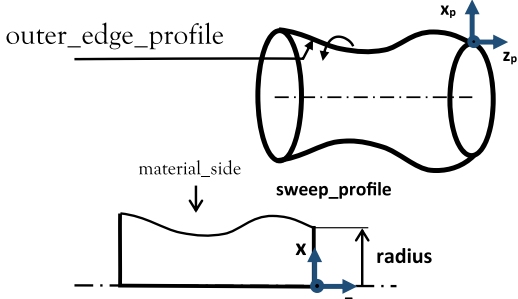
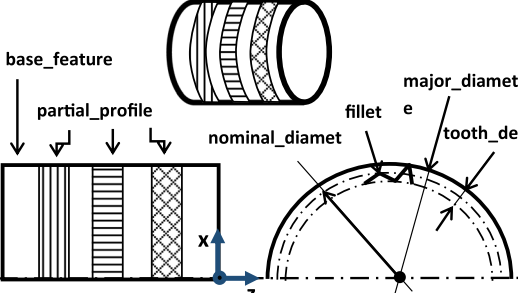
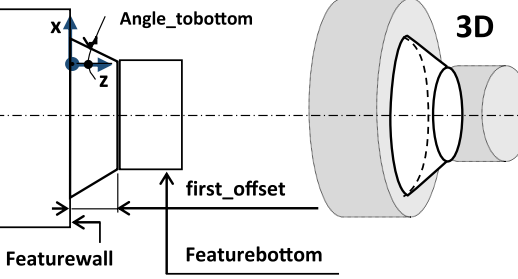
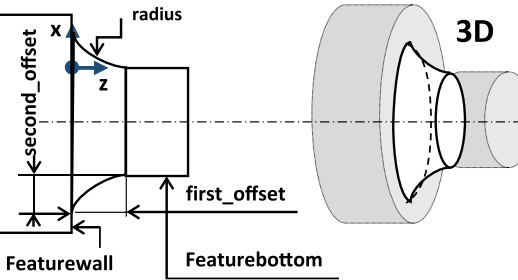
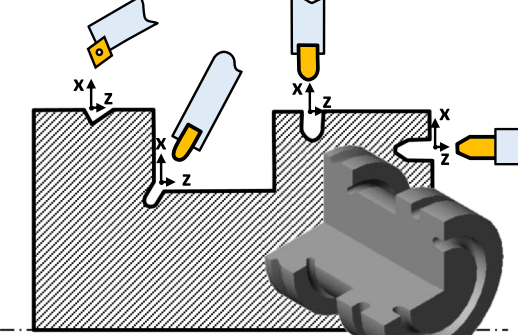
<p>general_revolution</p>	 <p>The diagram illustrates a general revolution. It shows an 'outer_edge_profile' which is a closed curve in the x_p-z_p plane. This profile is rotated around the z_p axis to create a 3D surface. A 'sweep_profile' is shown as a cross-section of this surface, with a 'material_side' indicated. The 'radius' is defined as the distance from the axis of revolution to the sweep profile. The axes x_p and z_p are shown in a coordinate system.</p>	<p>The profile concerned by the revolution must be finite, coplanar with the z axis and does not intercept this axis of revolution</p>
<p>Moletage</p>	 <p>The diagram shows 'Moletage' (knurling) on a cylindrical part. It includes a 'base_feature' and a 'partial_profile' of the knurling. Key parameters are labeled: 'nominal_diamet', 'major_diameter', 'fillet', 'e' (the height of the knurling teeth), and 'tooth_depth'. A coordinate system with x and z axes is provided.</p>	<p>Knurling can be considered as form work</p>
<p>Bottom_transition_slope</p>	 <p>The diagram illustrates a 'Bottom_transition_slope' on a cylindrical part. It shows a cross-section with a sloped bottom edge. Parameters include 'Angle_tobottom', 'first_offset', 'Featurewall', and 'Featurebottom'. A 3D view of the part is shown to the right. A coordinate system with x and z axes is provided.</p>	<p>Feature Wall and feature bottom are turning entities. For example: cylinder and plane</p>
<p>Bottom_transition_round</p>	 <p>The diagram illustrates a 'Bottom_transition_round' on a cylindrical part. It shows a cross-section with a rounded bottom edge. Parameters include 'radius', 'second_offset', 'first_offset', 'Featurewall', and 'Featurebottom'. A 3D view of the part is shown to the right. A coordinate system with x and z axes is provided.</p>	<p>Feature Wall and feature bottom are turning entities. For example: cylinder and plane</p>
<p>Bottom_transition_slope</p>	 <p>The diagram shows a 'Bottom_transition_slope' on a cylindrical part. It includes a 3D model of the part and a cross-section showing the sloped bottom edge. A coordinate system with x and z axes is provided.</p>	<p>Feature Wall and feature bottom are turning entities. For example: cylinder and plane</p>

Fig. 10 Outer diameter class and its attributes

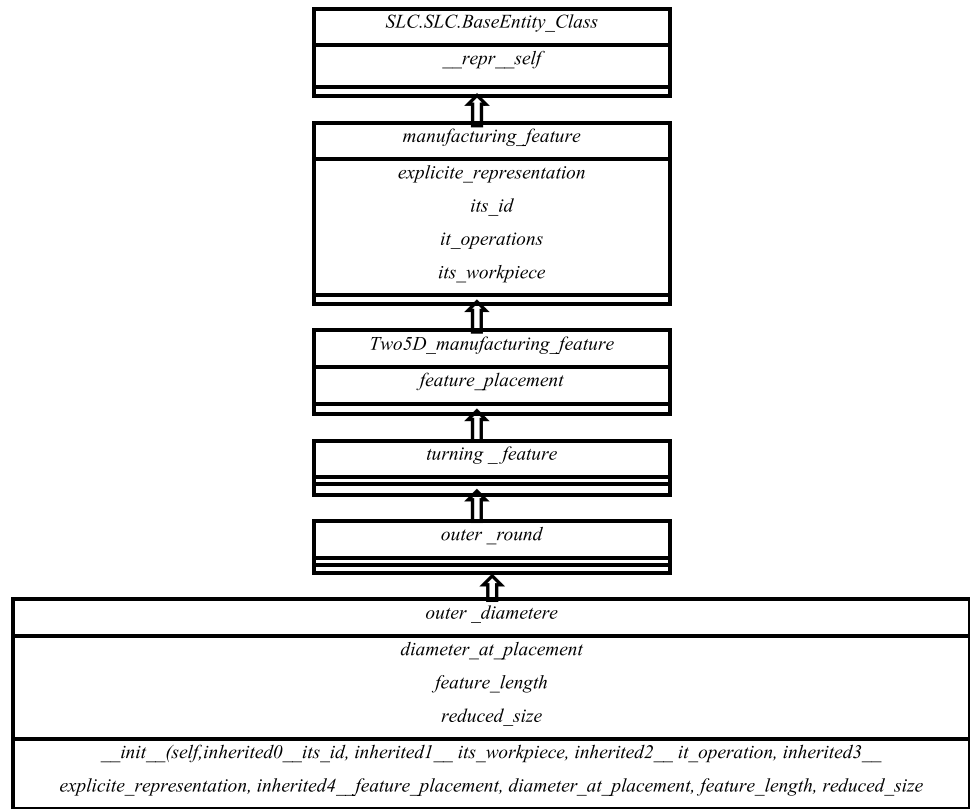
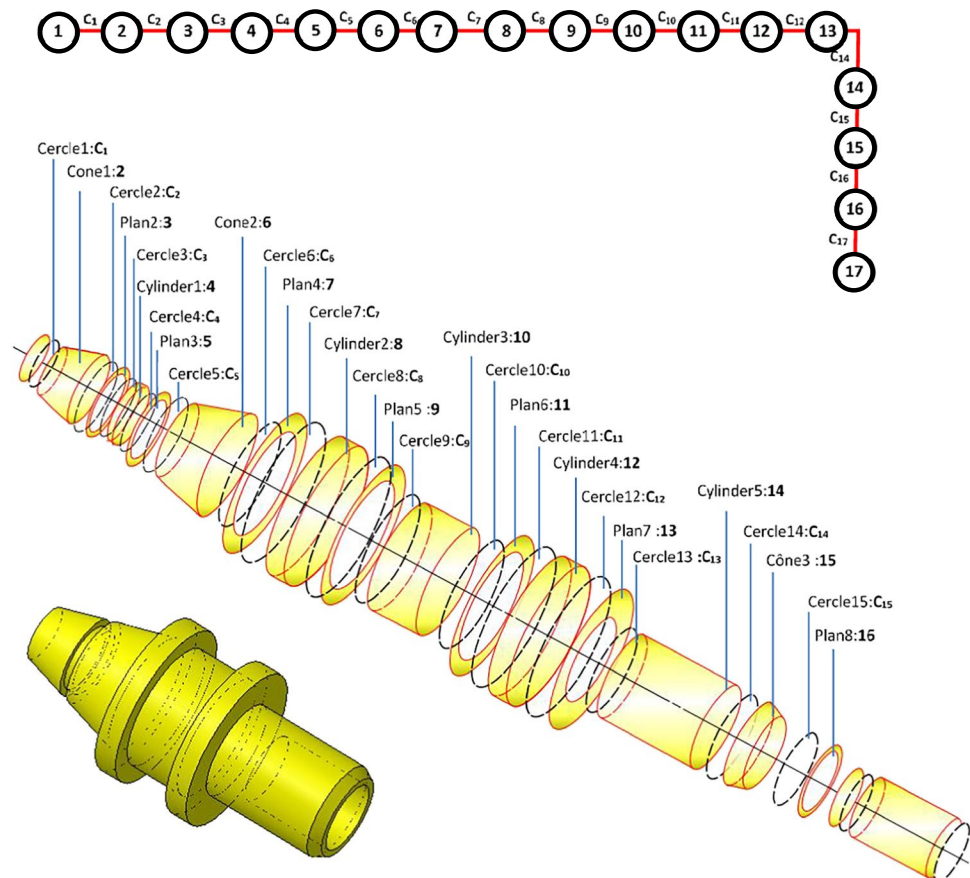


Fig. 11 Modeling of parts of revolution by series association of elementary entities



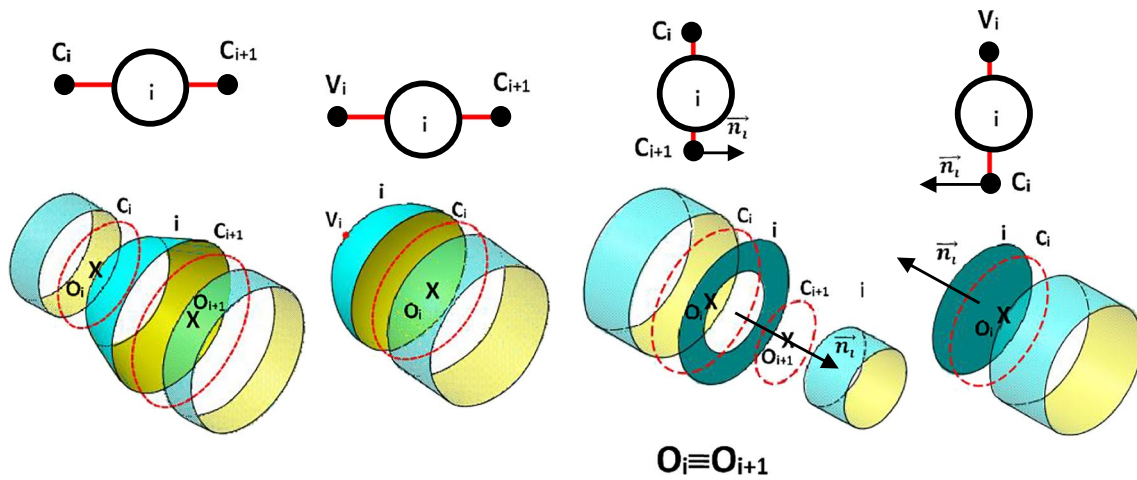


Fig. 12 Elementary graphs of different types of entities that can appear in symmetrical cylindrical parts

of the part. Faced with this situation and in order to facilitate the machining operation of the part, it becomes necessary to translate all the dimensions related to the part to be turned into a local coordinate system identical to that of the three-axis CNC numerical control machine, and taking into account the scale factor (Fig. 14).

We define the part’s CAD model coordinate system as the main base. This reference system is completely defined in the CAD STEP file of the part in question: its origin O is of coordinates $(0, 0, 0)$, and its direction vectors, defining its three axes, are $\vec{x} = (1, 0, 0)$, $\vec{y} = (0, 1, 0)$, and $\vec{z} = (0, 0, 1)$.

The local system linked to the part and which, in principle, should be identical to that of the CNC lathe machine is constructed as follows:

The center of the extreme face of the part of revolution will be taken as the local reference center (O_1 or O_2). By convention, we take the center closest to O , or O_1 . This center is defined by the vector \vec{OO}_1 .

The Z_p axis of the cylinder is given directly by the part’s STEP file. In fact, for each elementary entity of the part, STEP defines this reference mark as follows:

The center of the O_{cyl} cylinder is given by the attribute:
 # Address=CARTESIAN_POINT ('Axis2P3D Location', (X_{cyl} , Y_{yl} , Z_{cyl}));

The direction of the entity’s Z_p axis is given by the attribute:
 # Address=DIRECTION ('Axis2P3D Direction', (X_z , Y_z , Z_z));

The direction of the entity’s X_p axis is given by the attribute:
 # Address=DIRECTION ('Axis2P3D XDirection', (X_x , Y_x , Z_x)).

The third Y_p axis will be defined from the cross product to form a direct orthonormal coordinate system: $y_p = \vec{z}_p \wedge \vec{x}_p$

Once the local coordinate system linked to the part of revolution is completely defined, each surface point defined in the main coordinate system will be brought back to the local coordinate system using the passage matrix between the two references:

$$\begin{bmatrix} X_1 \\ Y_1 \\ Z_1 \end{bmatrix} = s \begin{bmatrix} X_X Y_X Z_X \\ Y_Z, Z_X - Y_X, Z_Z, X_X, Z_Z - X_Z, Z_X, X_Z, Y_X - X_X, Y_Z \\ X_Z, Y_Z, Z_Z \end{bmatrix} \cdot \begin{bmatrix} X \\ Y \\ Z \end{bmatrix}$$

3.5 Dimensionality reduction for the representation of the part

To simplify the processing of the information and the algorithms that will be used for the extraction of the entities and the definition of their machining strategy in a later step, again, we will use the properties of axial symmetry characterizing the parts of revolution to reduce the dimensionality from 3D CAD representation to 2D CAD. This step is facilitated by the existence of loops surrounding each surface and the geometric/topological definition of each edge forming the loop. Thus, in this way, the cylinder and the cone will be represented only by their generator, the circular plane by the radial segment coming from the center of the circle delimiting the plane and the point belonging to the circle, the spherical end piece by its circular arc, and so on. Likewise, the circles of connection between entities will be reduced to points of connection. It should be noted that all 2D entities are arranged so that they are contained in the same representation plane.

From the moment when the entity identification is carried out, we can reduce the 3D dimensionality to two dimensions by fixing the axis of rotation of the part and

Fig. 13 Flowchart for extracting a simple cylinder feature

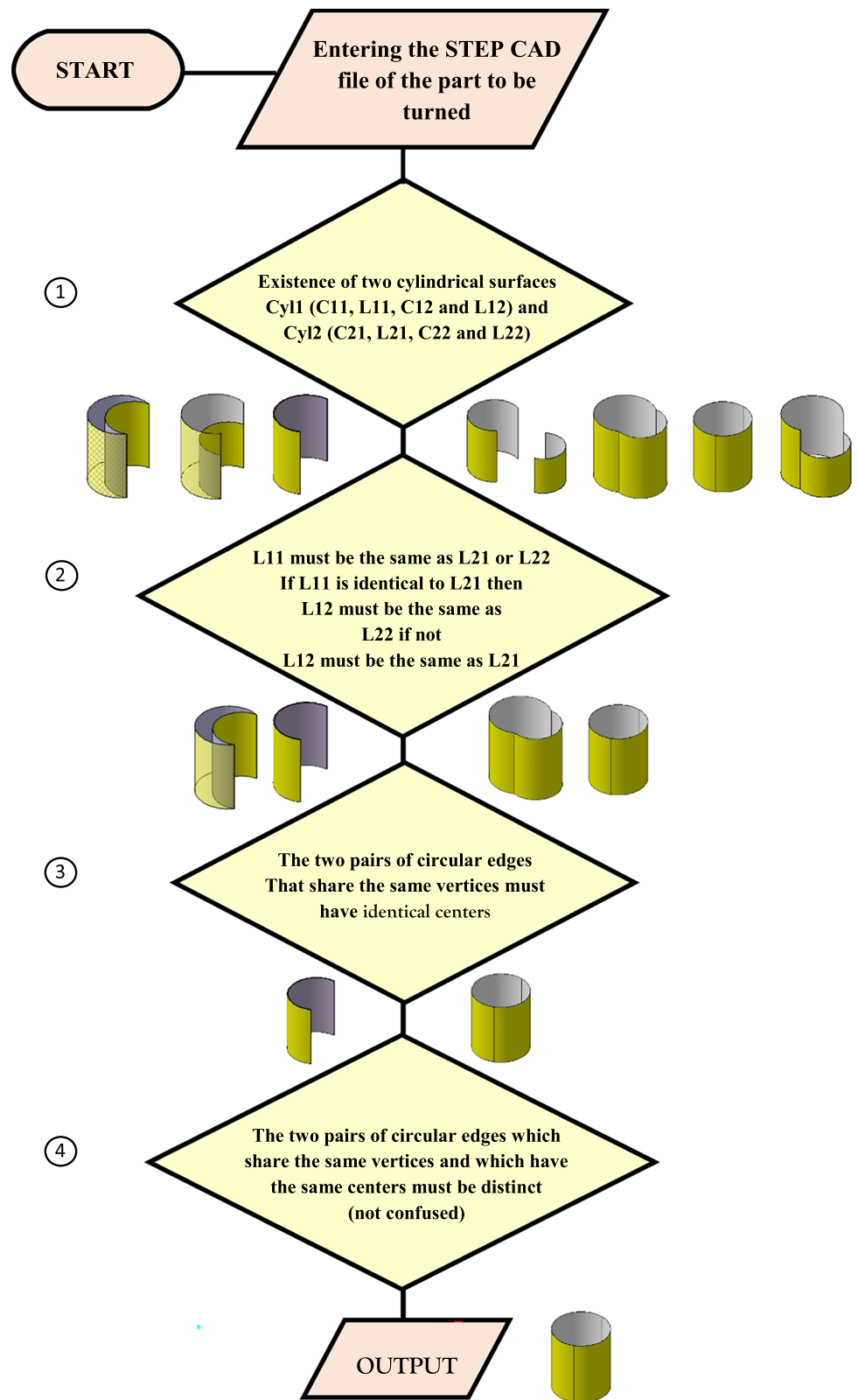
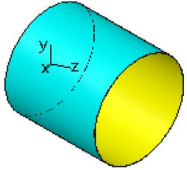
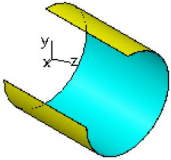
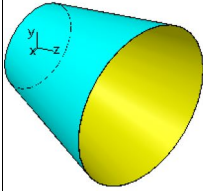
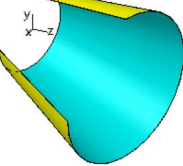
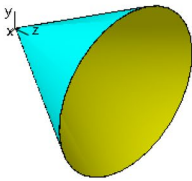
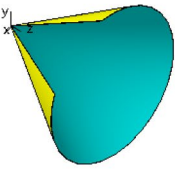


Table 3 Detection rules for basic external and internal entities

Name of entity	Entities	Entités	Entity recognition rules
Cylinder			<ol style="list-style-type: none"> 1. Existence of two cylindrical surfaces Cyl1 and Cyl2 delimited respectively by two loops Loop1 (ArcCirc11, Line11, ArcCirc 12 and Line12) and Loop 2 (ArcCirc 21, Line21, ArcCirc 22 and Line22) 2. Line11 must be the same as Line21 or Line22 If Line11 is the same as Line21 So Line12 must be the same as Line22 if not Line12 must be identical to Line21 3. The two pairs of circular edges that share the same vertices must have identical centers. 4. The two pairs of circular edges which share the same vertices and which have the same centers must be distinct (not confused)
Cone			<ol style="list-style-type: none"> 1. Existence of two Conical surfaces Cone1 and Cone2 delimited respectively by two loops Loop1 (ArcCirc11, Line11, ArcCirc 12 and Line12) and Loop 2 (ArcCirc 21, Line21, ArcCirc 22 and Line22). 2. Line11 must be the same as Line21 or Line22 If Line11 is the same as Line21 So Line12 must be the same as Line22 if not Line12 must be identical to Line21 3. The two pairs of circular edges that share the same vertices must have identical centers. 4. The two pairs of circular edges which share the same vertices and which have the same centers must be distinct (not confused)
			<ol style="list-style-type: none"> 1. Existence of two Conical surfaces Cone1 (Line11, ArcCirc1 and Line12) and Cone2 (Line21, ArcCirc2 and Line22). 2. Line11 must be the same as Line21 or Line22 If Line11 is the same as Line21 So Line12 must be the same as Line22 if not Line12 must be identical to Line21 3. The two pairs of circular edges ArcCirc1 and ArcCirc2 which share the same vertices must have identical centers. 4. The two pairs of circular edges ArcCirc1 and ArcCirc2 which share the same vertices and which have the same centers must be distinct (not confused)

by retaining, for each elementary entity detected, only the 2D profile from which this entity was generated by revolution. This will, on the one hand, save memory and, on the other hand, facilitate and accelerate the rapid processing of data. The dimensionality reduction operation is carried out directly from the STEP AP203 file using the loop delimiting one of the two surfaces of the elementary entity concerned. In practice, to extract the 2D entity, we will fix a single surface among the two surfaces forming the elementary entity (cylinder case). Knowing that each

surface of an entity is surrounded by a loop composed of two circular arcs (sometimes a point and a single arc when the surface is at the end of the entity, e.g., a cone with a pointed vertex) and two parallel 2D curves of the same type characterizing the surface nature of the entity (a line // to the axis in the case of a cylinder), by reason of symmetry, the cylinder can be represented by only one of the two non-circular curves (lines) bounded by two vertices which are the image of its two adjacent starting circular arcs (or else an arc and a point). However, for more

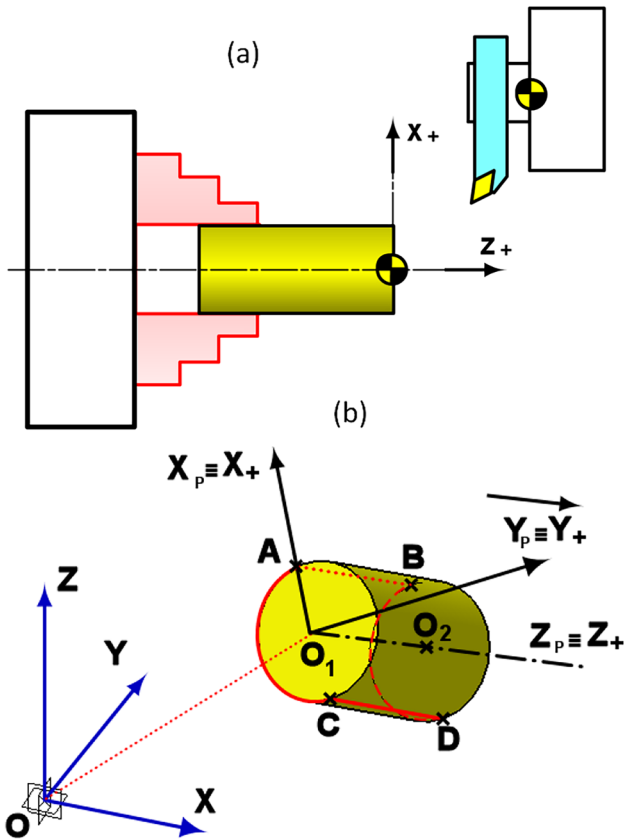


Fig. 14 Three-axis CNC machine mark (a) and CAD part mark (b)

structuring, this substitution approach must respect the 2D series association isomorphism graph established from the 3D one described previously. The transition from the 3D graph to the 2D graph is done as follows:

- For each pair of non-circular profiles of the loop delimiting one of the two fixed surfaces forming the elementary entity, we associate a profile representing among the two profiles of the loop.

Fig. 15 Elementary graphs of different types of 2D entities that can be present in a revolved part

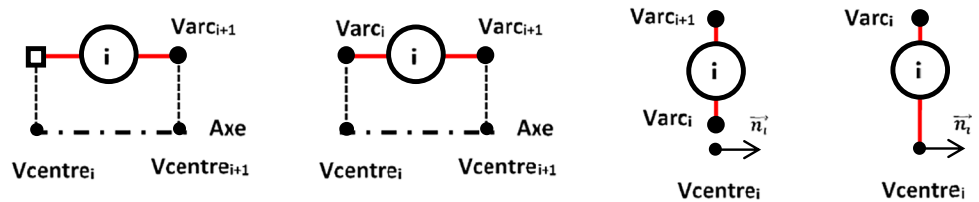
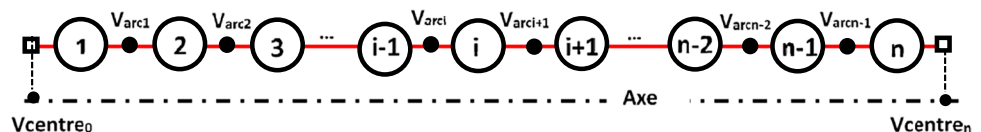


Fig. 16 Graph model obtained by series association of the different elementary features of the turned part



- Knowing that each element of the pair of arcs of a loop is delimited by two Vertex StartArc and FindArc, we associate with each element of the pair of arcs, among StartArc and FindArc, only two vertices: the first represents the adjacency vertex of the arc with the chosen non-circular profile, and the second represents the center of this arc.

Finally, an elementary entity i will be modeled in two dimensions by (1) a numbered vertex i representing the 2D curved entity of the initially extracted entity I and (2) two pairs of vertices $(Varc_i, Vcentre_i)$ and $(Varc_{i+1}, Vcentre_{i+1})$. $Varc_i$ and $Varc_{i+1}$ define the limits of the 2D curve and are at the same time the images of the two adjacent circular arcs upstream and downstream of this curve, and $Vcentre_i$ and $Vcentre_{i+1}$ define the axis of revolution from which the elementary entity was generated by revolution of the corresponding 2D curve (Fig. 15). It is important to note that the two vertices $Varc_i$ and $Varc_{i+1}$ will be respectively the possible points of adjacency (of connection) of the entity i with its predecessor $i - 1$ and its successor $i + 1$.

For the construction of the total isomorphism graph of the part in 2D mode from 3D, (1) we replace each surface entity i by its profile i from which this entity was generated, and (2) we replace each circle C_i of junction between the entity i and $i + 1$ by the pair of vertices $(Varc_{i+1}, Vcentre_{i+1})$. Finally, the modeling of the final part is a series association of elementary 2D entities connected by fusion of the common vertices as shown by the isomorphism graph of Fig. 16 below:

For the construction of the total isomorphism graph of the part in 2D mode from 3D, (1) we replace each surface entity i by its profile i from which this entity was generated, and (2) we replace each circle C_i of the junction between the entity i and $i + 1$ by the pair of vertices $(Varc_{i+1}, Vcentre_{i+1})$. Finally, the modeling of the final part is a series association of elementary 2D entities connected by fusion of the common vertices as shown by the isomorphism graph of Fig. 17 below:

Fig. 17 Diagram for determining the linear curve for the generation by revolution of a simple cylinder



3.6 Differentiation between interior and exterior entities by dressing the graph

3.6.1 Situation

The differentiation between external and internal entity is a decisive stage for the constitution of internal and external turning entities since their method of machining can be distinguished between the two types. Much research has dealt with their CAPP systems only with exterior turning and have neglected interior turning despite the need for complete machining of parts [10, 11, 29, 33, 34]. The algorithms used to classify a machining entity as an interior entity (depression) are few in number and are the basis of rules [35–37], image processing [38], ridge orientation [30]

and the concavity of the edge shared between the entity and its bearing surface [39].

To isolate the interior entities from the exterior entities, we will rely on a careful reading of the CAD file STEP AP203 of the part. It is recognized that STEP AP203 largely preserves the information of the initial B-Rep model (geometry and topology). Recalling that a massive part is modeled, within the framework of this format, by the entity shell which is delimited by its border surfaces, the difficulty in identifying protrusions and depressions for a given room is the existence of great similarity between the two in terms of type of surfaces and topology. Thus, a protrusion formed by a cylinder and a depression formed by a hole (Figs. 18, 19) are both defined by the same type of cylinder surface and are both surrounded by two circular loops, BInt and BExt. Without the use of other

Fig. 18 Comparison of a cylindrical protrusion and a cylindrical depression on the basis of their geometric and topological definitions

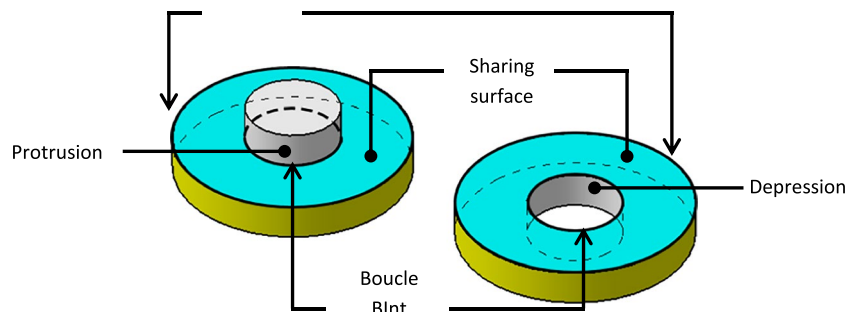
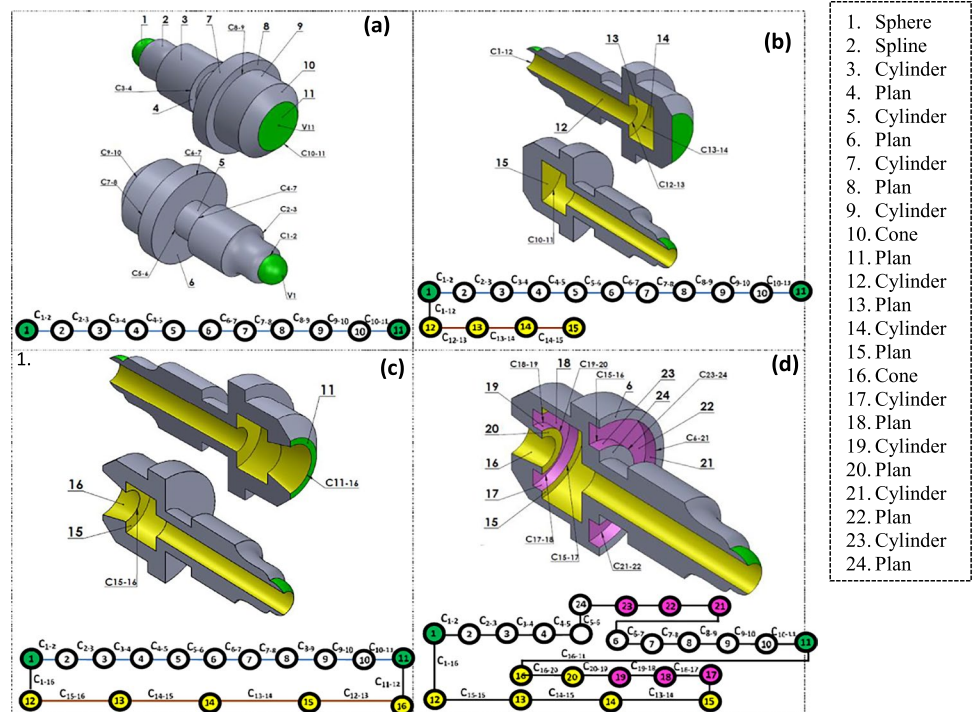


Fig. 19 Categories of turned parts and their isomorphism graphs



attributes of these two entities, such as concavity, identification becomes very difficult.

In what follows, the term depression designates, for us, a cavity which has an entrance (or an exit for the emerging cavities) and which can be formed by several types of surfaces of revolution chained in series (like a cave) from the entry of the cavity to its end. On the other hand, all the surfaces in series forming the cavity necessarily have the same axis of symmetry.

In the previous work developed by our PhD student Ousama Jaider, a system called CAPP-Turn was designed taking advantage of the performance of the two standards STEP and STEP-NC. This system is made up of four modules:

Module 1: This module translates the geometric and topological information contained in the part's STEP AP203 CAD file, written in the EXPRESS language, into Python entity classes. In a second step, it maps entity instance parameters to Python class attributes. Mapping scripts are developed for each class in order to establish a link between its parameters and its attributes.

Module 2: This module is an autonomous system of automatic recognition of turning entities which consists in analyzing the objects created (surfaces: geometry and topology) and applying rules (rule-based approach) to construct machining entities based on a library of predefined feature classes.

Module 3: In the third module, an entity combination generator (ECG) is developed. This system analyzes

the boundary surfaces of entities to decide whether the extracted entity is simple or interacting. The interacting entities are transformed into simple entities by extrapolation from their material surfaces to the stock surface. The elaborate system allows multiple interpretations of entities to be generated, leading to a range of part machining sequencing choices.

Module 4: In the fourth module, two systems are designed, one called entity eliminator (EE) and the other shoulder generator (GE). The first system consists in excluding a few unwanted ranges, generated by the GCE module, based on the manufacturing rules and the principles of material removal. This considerably reduces the number of entity interpretations. The second system presents a new approach to remedy the drawbacks of the method of extrapolation of module 3, in particular in the presence of the shoulders interacting at a non-right angle. This previous work was focused on the case study of parts with simple basic entities or in the best case with shoulders in mutual interaction, in order to give more interest to the implementation of the new STEP-NC standard and facilitate its integration. Also, the algorithms used in the entity recognition step (core of the system) have been restricted to exterior filleting. From this perspective, these algorithms deserve to be reviewed to bring more structure to the system and also to deal with the cases of turning parts presenting internal entities and complex profiles.

3.7 Differentiation between interior and exterior entities by dressing the graph

The turning part is expressed by the following model:

$$\text{Turning part} = \text{External features} + \text{Internal features}$$

Exterior Features of a Part = A series association of surfaces that includes exterior side surfaces, exterior front surfaces, exterior radial depressions and exterior frontal cavities.

Interior Features of a Part = A series association of surfaces that includes interior side surfaces, interior front surfaces, interior radial depressions and interior frontal cavities.

It should be noted that the two interior and exterior parts of the room are linearly independent and are connected on the left by the adjacency circle located at the extreme bottom left of the room. Similarly, on the right, these two parts share the adjacency circle located at the extreme bottom right of the same room.

a. First reading of the isomorphism graph of a turning part Figure 20 a–d present the main machining features which may appear on a turning part: the exterior surfaces, the interior bores, terminals and outlets executed along the axis, the front exterior and interior depressions.

The representation of this category of cylindrical parts by the graph method, described previously, makes it possible to highlight two types: the first type is an open graph made up of a series association of surfaces linked by circles of adjacency (Fig. 19a and b).

The second type is described by a closed graph (Fig. 20c and d) composed of a continuous sequence of surfaces in a loop formed.

Our methodology consists of first identifying the cavities of a frontal nature that exist on the part and then eliminating them, as these cavities complicate the process of recognizing features of the part. Without the presence of these cavities, we will only have the cases of parts presented in Fig. 20a–c.

b. Mathematical concepts, definitions and terminologies Before approaching the analysis for the differentiation of the external entities from the internal entities, it will be interesting to introduce some definitions and terminologies which will be used to describe the method we are going to adopt:

b.1 Definition of the tree of a graph

A tree is a continuous path extracted from the graph of the part, such that by traversing it, we do not encounter the same vertex twice: in our case, it is an open chain of surfaces connected two-by-two by circles of adjacencies

Principle of surface encapsulation Given two adjacent surfaces F and G of a turning part and their associated curves of revolution f and g, the function f is defined on the interval

Fig. 20 Encapsulation criterion between two adjacent surfaces of a turning part

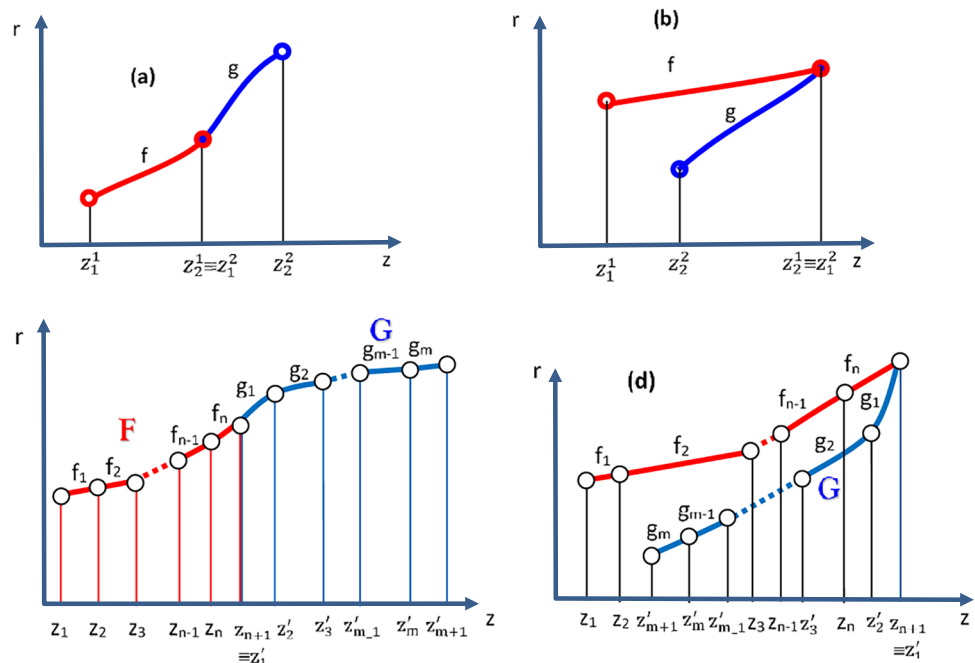
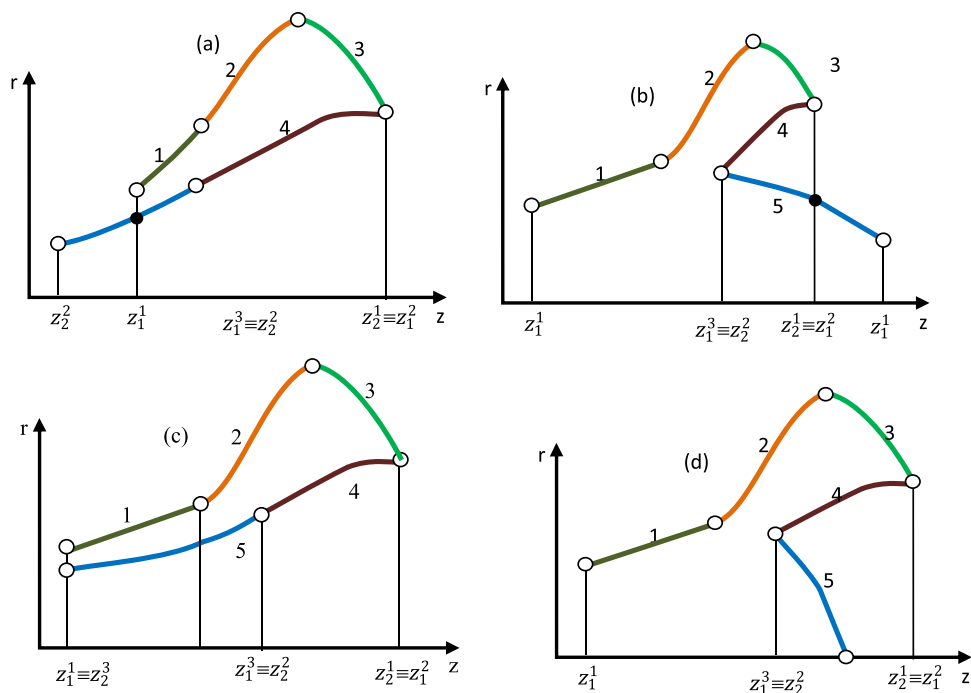


Fig. 21 Different types of encapsulations of surfaces of revolution



$[z_1^1, z_2^1]$ and g on $[z_1^2, z_2^2]$ and they share the adjacency point of abscissa $z_2^1 \equiv z_1^2$. The entity f/F can encapsulate g/G (and vice versa) only if the two functions are of different monotony, i.e. one is increasing and the other is decreasing. Thus, in the case of Fig. 20a, f/F cannot encapsulate g/G because the two functions f and g are strictly increasing. On the other hand, in the case of Fig. 20b, f covers g because f is strictly increasing and g is strictly decreasing. The same reasoning remains valid if F and G consist of a set of n surfaces, arranged in series and with the same monotony: $F = \{F1 + F2 + \dots + Fn\}$ and $G = \{G1 + 2 + \dots + Gm\}$ Fig. 20c and d.

The encapsulation of surfaces can be full or partial, simple or multiples. Figure 21a and b show a partial encapsulation where the functions $1 + 2 + 3$ partly encapsulate $4 + 5$. The encapsulation in Figs. 22, 23a is simple because it is made only once per f , while this encapsulation, Fig. 21b, is multiple (double) because entity 5 is covered twice: firstly, by entity 4 and secondly by entities $2 + 3$. In the same way, Fig. 21c presents a type of full-simple encapsulation, and Fig. 21d a full- multiple encapsulation.

b.2 Classification of the different trees of a graph
 Different trees can coexist in the total graph of the part, as shown in Fig. 22:

- AEEL lateral exterior entity tree: formed by a series chaining of lateral exterior surfaces which are not

encapsulated by any other surface (Tree 1, Tree 41, Tree 34, Tree 30², and Tree 24–25–26).

- AEEF frontal external entities made up of a series association of frontal external entities which may or may not include external frontal depressions (Tree 23, Tree 2–31, Tree 42–43–44–45, Tree 35–36¹, Shaft 37–38–39–40, Shaft 30³–31–32–33 and Shaft 27–28–29–30¹).
- AEILA axial lateral interior entity that consists of a series chaining of axial lateral interior surfaces. These constituent surfaces do not encapsulate any other surface (Tree 41, Tree 8–9, 102, Tree 14, Tree 16 and 22²).
- AEIF frontal interior entity tree: formed by a chain of frontal interior entities which may or may not include interior frontal depressions (Tree 15, Tree 4²–5–6–7, Tree 10¹–11–12–13 and the Tree 17–18–19–20–21–22¹).
- AEID breakthrough internal entity tree: formed by a series of AEILA and AEIF series which opens out on both sides of the room.

AEIB terminal inner entity tree: formed by a series chaining of AEILA and AEIF which emerge from one side of the room.

AEE: external entities formed by a serial association of AEEL and AEEF (example: Tree 23–24–25–26).

b.3 Differentiation between internal and external turning entities

Fig. 22 Different types of graph trees for a cylindrical part

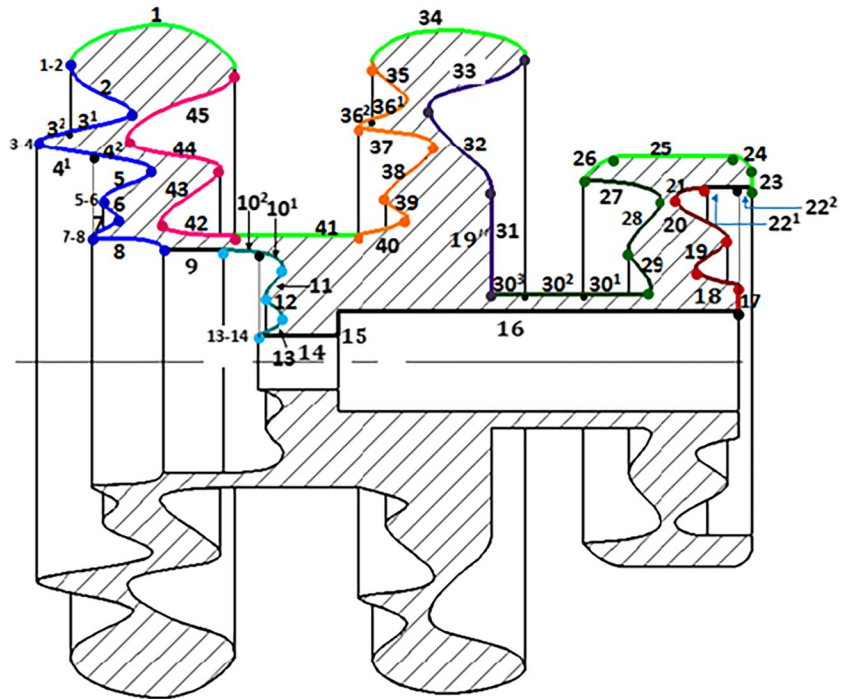
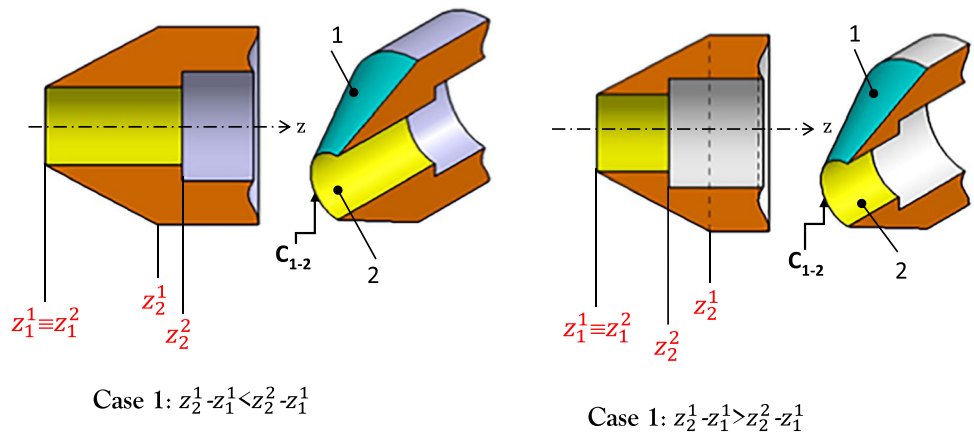


Fig. 23 Differentiation between exterior and interior features



Identification of an internal entity tree AEIB terminals:
 When the graph of the part is open and there is only one entity at the end of the graph that coincides with one of the two entities at the end of the part, we will have the presence of an AEIB. If the two coincide, there are two AEIBs. It is necessary to specify that in the case of an open graph of parts with terminal axial cavities, the start of the cavity and its end are fully identified when the end of the graph is associated with its axial position in the part.

Identification of an AEID entering internal entity tree:
 Unlike solid parts or solid parts that have one or two AEIBs, axially open cavity parts are identified by a closed

loop graph. Although for this category of parts the two ends of the through axial cavity can be given from their position, the shaft corresponding to this depression cannot be identified because the end corresponds to a point of adjacency shared between this shaft (interior nature) and another exterior type tree. To solve this problem, we are going to proceed to a section, well chosen, offset axially with respect to each end. Indeed, in Fig. 23, the two entities 1 and 2 share the circle of adjacency C1-2.

In case 1, since the abscissa z_2^2 of the end circle of entity 1 is less than the abscissa z_2^2 of entity 2, for simplicity, the radius comparison section is chosen at this position.

For the same reason, this comparison is maintained at the position for case 2. For case 1 where $z_2^1 - z_1^1 < z_2^2 - z_1^1$, if the radius of entity 1 corresponding to the axial position z_2^1 is greater than the radius of the section of 2 executed at the same position, we conclude that the entity 1 is the strictly encapsulating surface of exterior nature, and 2 is the interior surface encapsulating of interior type. Otherwise, 2, the same procedure is to be applied only the section will be executed this time to element 1 at position z_2^2 .

The calculation of the radii, at the section chosen, depends on the nature of the envisaged surface. Table 4 summarizes the different necessary mathematical formulations established to approach this calculation. Since the B-spline curves used in the revolution operation are specific parameterized curves, we use the approach presented in Appendix Table Six for the calculation of the radius of the entity chosen at the specified section, and this in relation to the data provided by the STEP file for this type of curve. The established algorithm has been programmed and tested using Maple V 11 software.

b.4 Detection of interacting frontal depressions

Frontal depressions can be exterior or interior in nature, as previously indicated in both Figs. 20d and 24. Exterior frontal depressions are part of the AEE outer entity trees, while interior frontal depressions are a subclass of AEIB/AEID. These entities, when interacting with other entities of a different type, greatly complicate their identification and the sequencing of their machining. Thus, it will be important to draw up a method allowing one to analyze these overlapping entities with a view to sharing them into simple entities easily recognizable by applying the rules formulated previously.

b.4.1 Mathematical formalism

Given a surface F of any type of a part of revolution and G its adjacent surface (Fig. 24 below).

Let $f = f(z)$ and $g = g(z)$ be the two curves used respectively for the generation by revolution of the two surfaces F and G . The function f is defined on the interval $[a, b]$ and g on $[c, d]$. Knowing that $f = f(z)$ and $g = g(z)$ are two monotonic functions (increasing or decreasing), if the two functions $f(z)$ and $g(z)$ have the same monotony (Figs. 25, 26a), then the two surfaces F and G cannot present a frontal depression (protrusion) at their junction point z_2 . Otherwise, a depression (protrusion) necessarily exists as indicated in Fig. 26b. In the same way as before, this reasoning can be extrapolated if we substitute F by $F_1 + F_2 + \dots + F_n$ and G by $G_1 + G_2 + \dots + G_m$.

b.4.2 Adaptation of the formalism in the detection of frontal depressions

Recalling that in our case a part is modeled by a graph of entities arranged in series. The mathematical formalism introduced can be applied without modification when all the generating functions by revolution associated with the different entities of the graph are monotonic. However, in the real case, a function associated with a surface is any function and can have parts of various monotonies. We proceed, in this case, to a discretization of the domain of definition of the associated function in intervals within which this function f keeps the same monotony. Each interval will be associated in the total graph of the part with a new sub-entity whose associated function is monotonic. Because of the assurance in advance of the monotony of all the functions associated with the polygon entities participating in the construction of the total graph of the part and to simplify the setting evidence of the change of direction in z direction characteristic of the presence of a depression/protrusion, we are going to traverse the graph entity by entity from a specific entity until its entire traversal. We will assign, for each entity i , an indicator of change in monotony quantified by the difference D between the abscissa z_1^i of its beginning and z_2^i the abscissa of its end (Fig. 25):

Next, we dress the top of each entity on the part graph with a + sign if d is positive, a – sign if d is negative and 0 if this indicator is zero.

Treatments for interacting frontal depressions:

This treatment is carried out for all linearly independent tree AEEFs identified from the part. The first tree identified is given by Fig. 26b.

The processing of external interacting front-end entities begins with entity 1 which is located at the extreme top left of the room, i.e., from the vertex materialized by the circle of adjacency $C_{1,2}$ (Fig. 26a). The general study of interacting frontal entities is established from Figs. 27, 28 above. We assume that for any entity i , the process of dealing with interacting entities is already established for all entities above it. Locally, the vertex i is seen as a point of connection of two entities of different nature: exterior i located above and interior $i + 1$ located below. The polygon entity $i + 1$ encapsulates all the polygon entities positioned below and to the right of vertex C_{i-i+1} . Only the entity j whose vertex is located on the left is partially encapsulated. This last entity marks, in fact, the end of the encapsulated surface chain and forms the second wall of the frontal depression. Therefore, the entity j will be separated into two zones: the portion j^d on the right side of C_{i-i+1} which is entirely encapsulated and the other free part on the left j^e which remains not covered by any surface. The latter will be declared as a surface sub-entity of

Table 4 Determination of the abscissa z of any section for specific features

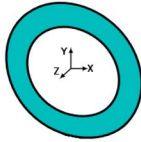
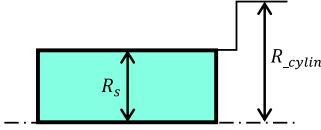
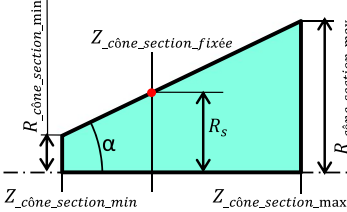
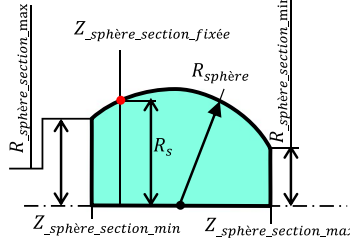
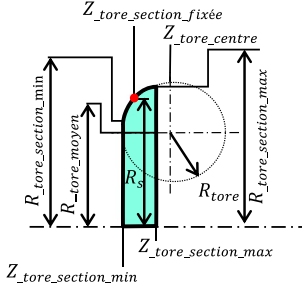
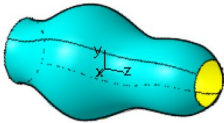
Name of entity	Entity	Formula for calculating the section radius at $Z_{fin_E_int}$ or $Z_{fin_E_ext}$
Plan		Without doing the test (no variation along z)
Cylinder		$R_{cylinder_section} = R_{cylinder} = cst$
Cone		$tg(\alpha) = \frac{R_{cône_section_max} - R_{cône_section_min}}{Z_{cône_section_max} - Z_{cône_section_min}}$ $R_s = R_{cône_section_cherchée}$ $= tg(\alpha) \cdot [Z_{cône_section_max} + Z_{cône_section_fixée}] - Z_{cône_section_min}$
Sphere		$Z_{sphère_centre} = Z_{sphère_section_min} - \sqrt{R_{sphère}^2 - R_{sphère_section_min}^2}$ $R_s = \sqrt{R_{sphère}^2 - [Z_{sphère_section_fixée} - Z_{sphère_centre}]^2}$
Torus		$Z_{tore_centre} = Z_{tore_section_min} - \sqrt{R_{tore}^2 - R_{tore_section_min}^2}$ $R_s = R_{tore_moyen} + \sqrt{R_{tore}^2 - [Z_{tore_section_fixée} - Z_{tore_centre}]^2}$
Spline		See the algorithm established in Appendix 2

Fig. 24 Criterion for the existence of a frontal depression between two adjacent surfaces of revolution

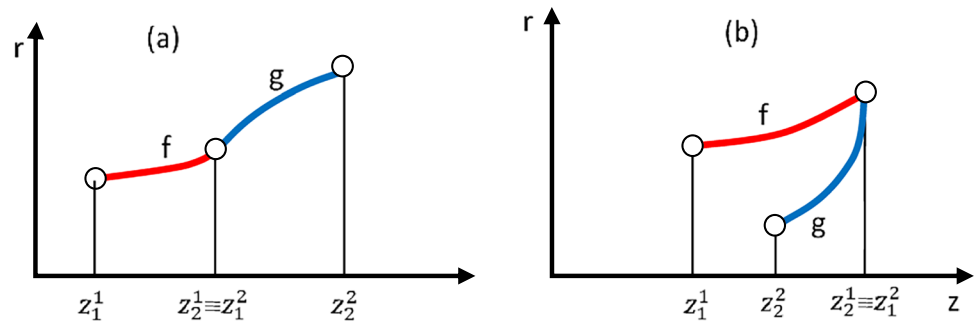


Fig. 25 Basic indicator to test for the presence of a depression/protrusion

$$D = z_1^i - z_2^i$$

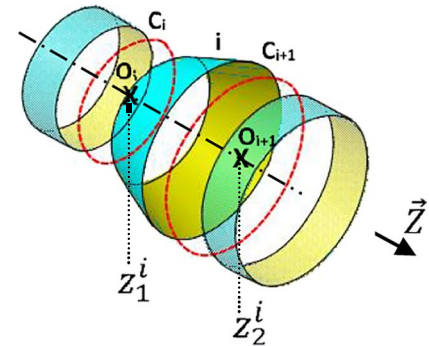
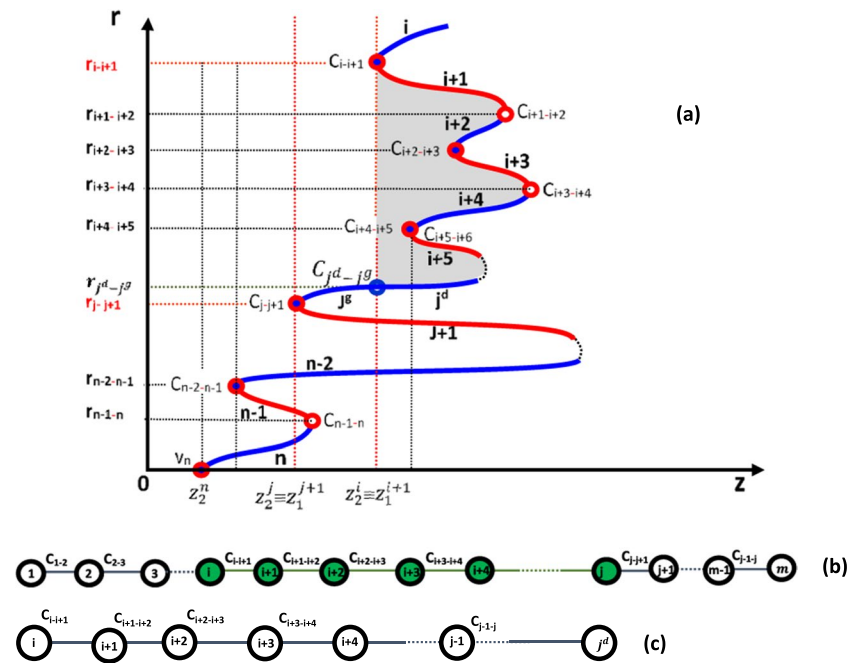


Fig. 26 Processing of frontal interacting entities of the external type



an external nature. The separation between the two entities is practically achieved by constructing the vertical plane surface (a matter of simplification which is in accordance with machining practices) lost by interaction during the

machining of the two entities. This new reconstituted frontal surface is delimited by the two circular loops C_{i-i+1} and $C_{j^d-j^s}$.

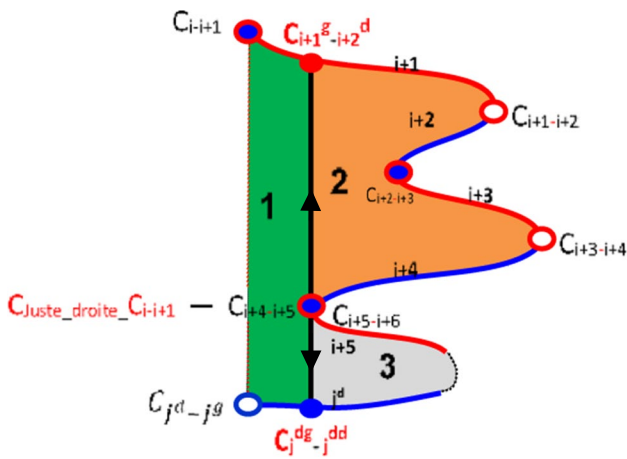
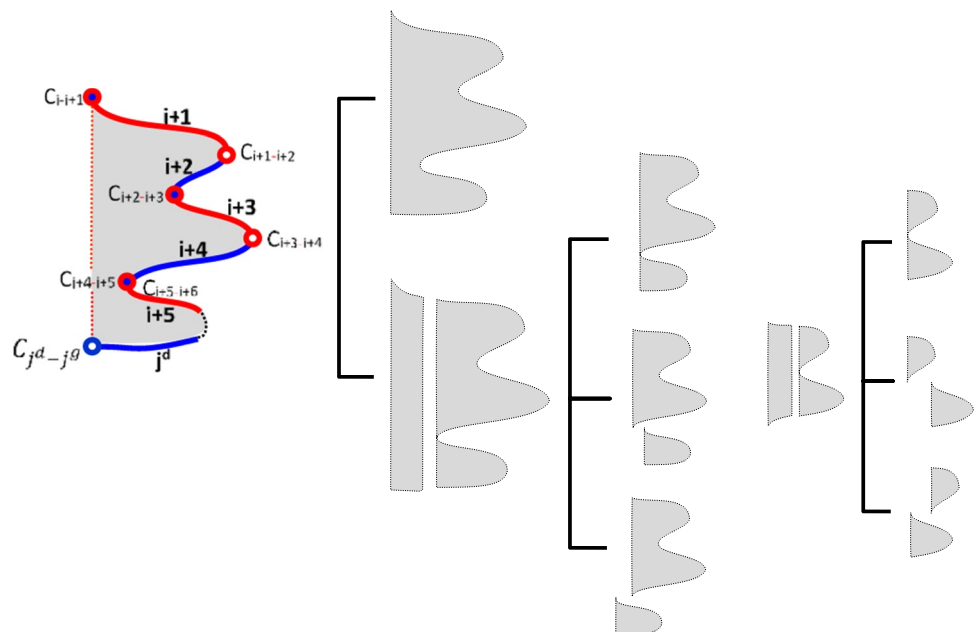


Fig. 27 Decomposition of the compound depression into simple elements

Finally, the desired frontal depression is given by the tree given in Fig. 26c. This depression is bounded by the two entities i and j^d .

This algorithm is repeated for the second branch (AEEF) connected on the left side of 1. Once the two front branches linked to 1 are processed, we go directly to the next AEELEG tree. This operation is ensured by removing from the total graph of the part the starting AEELEG and the treated front branch. The process ends just after processing the last front branch connected to the right of the AEELED tree.

Fig. 28 Possibilities for the sequencing of the machining of a compound frontal depression containing two peaks



Interacting frontal depression of the interior type:

The same reasoning is applied except that it is necessary to start with the first domain bounded by the strictly encapsulated interior surface located at the extreme top-left of the part (AEIAG) and the first entity found by following the graph which is of the same nature. The scanning process is also carried out from left to right up to the front branch located just before the last AEILAD tree in the part.

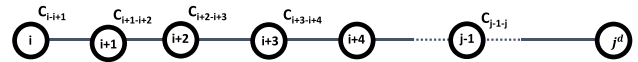
Filtration of simple frontal depressions of compound frontal entities:

Definition: A frontal depression is said to be simple if:

- a. it does not include any vertex between its two border vertices C_{i-i+1} and C_j ;
- b. the two vertices C_{i-i+1} and C_j are located at the same axial position.

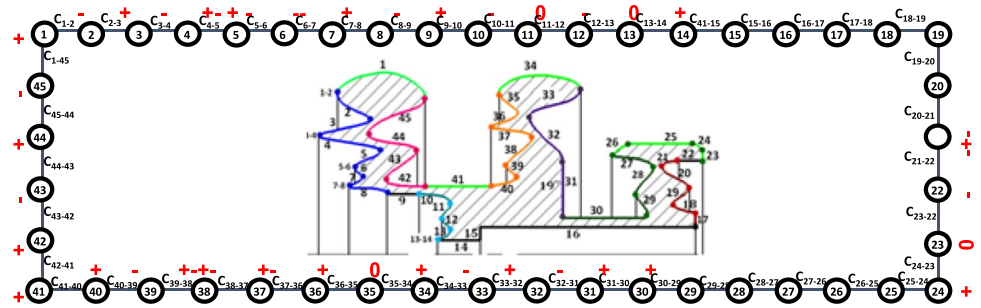
In case the depression includes several peaks like the depression treated above (Fig. 26), it is isolated to address its decomposition (Fig. 27):

This depression is given by the following tree:



Several ways of approaching its machining can be envisioned, and therefore its decomposition or not remains

Fig. 29 Dressed isomorphism graph of the example part considered



dependent on the method to be applied. In terms of productivity, it is advantageous to start a mass machining; in this case the shape machining using a tool with the desired profile is preferable. However, tool wear is one of the decisive factors in determining the choice. Casing machining can also be used when accessibility of the tool and a smooth and desirable surface condition are ensured. However, without privileging one method, we will be interested, in the following paragraph, in the generation of these different ways of executing this frontal groove and of its decomposition and its discretization into elementary elements as described in the figure above.

To begin machining by part of the front groove studied, the first material removal is carried out frontally up to the first ridge located just to the right of the vertex C_{i-i+1} (Figs. 28, 29). This will allow us to simplify the machining strategy and the profile of the tool to be used in case of form machining. This volume of matter is obtained by projecting radially the vertex just to the right of C_{i-i+1} onto the above faces $i + 1$ and top

face j^d (radial tangent to this vertex). This projection allows the subdivision of the entity $i + 1$ into two segments: one on the left $i + 1^g$ and the other on the right $i + 1^d$. In the same way the entity j^d is divided into two portions j^{dd} and j^{dg} , two new separation planes are created which are delimited respectively by the circle of adjacent C_{i+1}^g and C_j^{dd} and the one relative to the first projected vertex. Three volumes of material are therefore generated by the sectioning of this initial frontal depression: the first (1) consists of the loop section $C_{i-i+1} - C_{i+1}^g - C_j^{dd} - C_{i+1}^d$, the second (2) corresponds to the tree given by traversing the tree of the graph of the frontal pressure from C_{i+1}^g until $C_{juste_droite_C_{i-i+1}}$ (opposite direction of the path leading to C_{i-i+1}) and the third is given by the remaining section which is defined by traversing the tree of the graph of the frontal pressure from C_j^{dd} to $C_{juste_droite_C_{i-i+1}}$ (opposite direction of the path leading to C_j^g). Depression 1 is a simple depression and is subsequently removed from the subgraph of this entity.

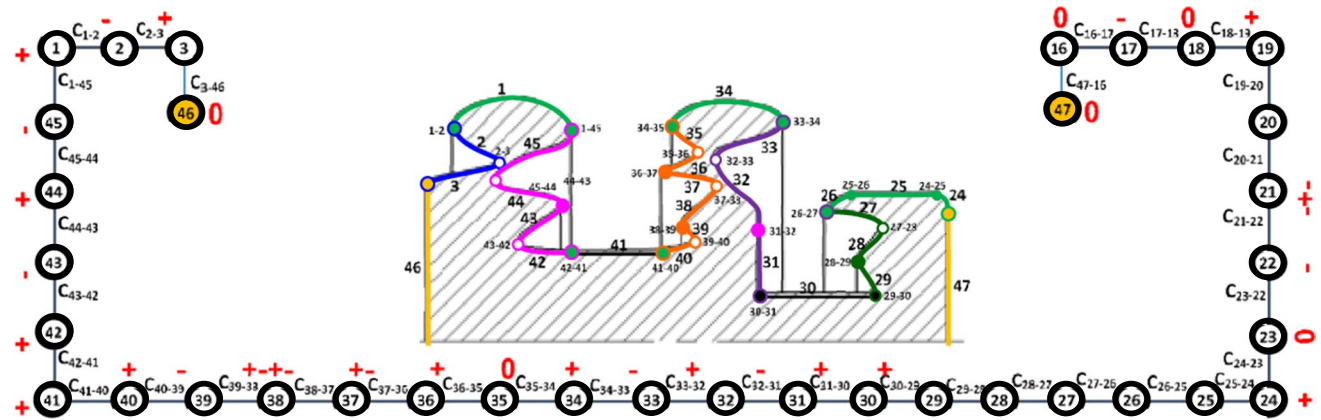
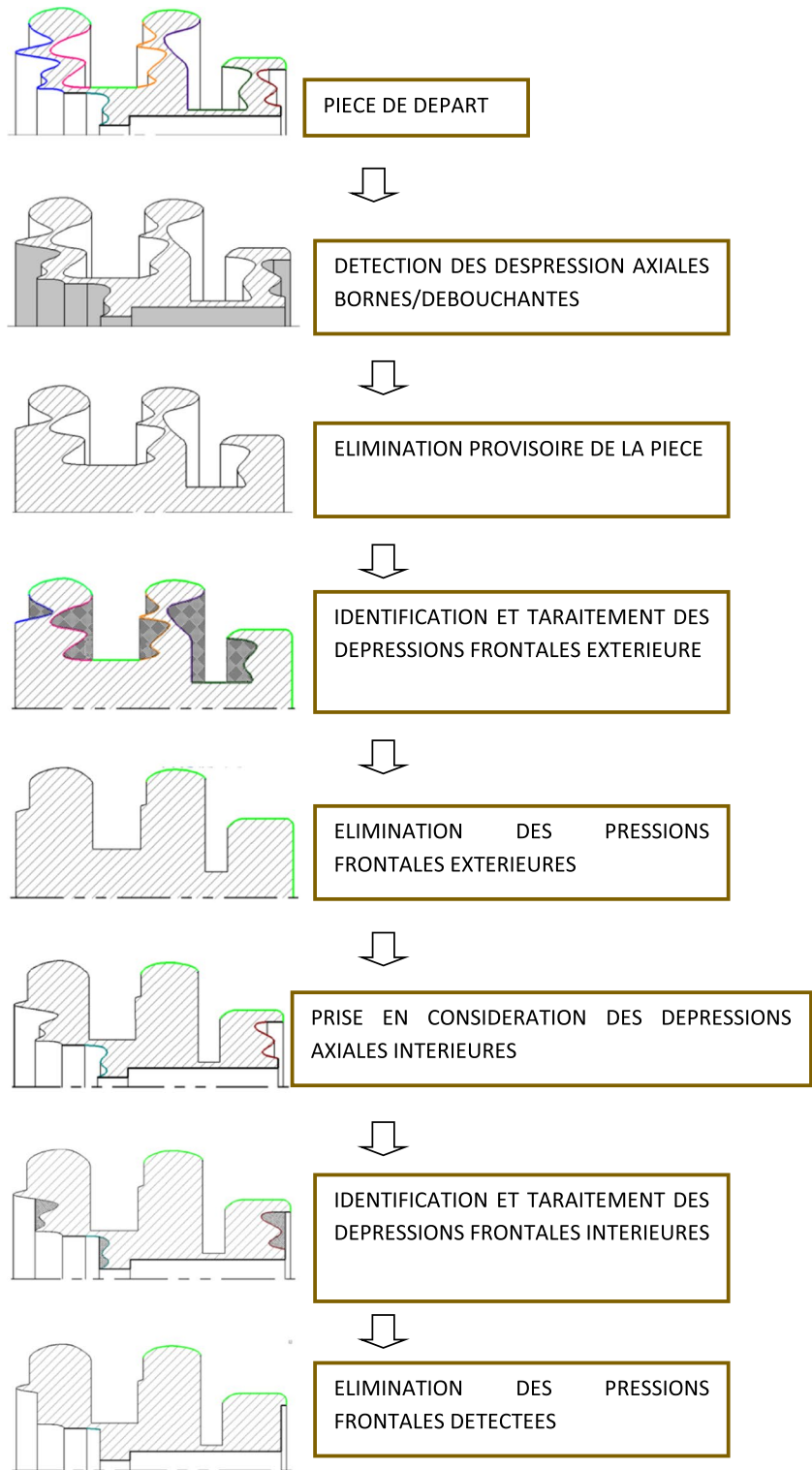


Fig. 30 New dressed isomorphism graph of the example part considered after elimination of the trees of the interior entities

Fig. 31 Organizational chart of recognition of filming entities



The algorithm is repeated for the two depressions 2 and 3 defined by their new graphs until there are only depressions of a simple nature. Figure 28 illustrates the different possibilities of interpreting the sequencing of the frontal depression studied by application of the developed method.

3.8 Summary of recognition procedure for different feature trees

The synthesis of the developed method to recognize the different types of trees existing in turning the part is given as follows:

1. Identification of the simple surface entities of the part.
2. Drawing of the part isomorphism graph (Fig. 29).
3. Study of the generating function by revolution of each non-standard surface entity and division into parts of curves which are monotonic.
4. Identification of the tree of the lateral exterior entity located at the extreme top left of the room: AEELEG.
5. Dressing of each surface entity of the graph by a + sign if its generating function by revolution is increasing, 0 if the entity is a vertical plane and – if it is decreasing. This skin is established by continuously scanning the graph (adjacent by adjacent) from the right end of the AEELEG to the end of the graph (Fig. 30).
6. Identification of terminal or through-axial depressions with the algorithms established for this object.
7. Elimination of the trees of these depressions to facilitate the identification of the exterior frontal depressions and addition of two vertical planes delimited respectively by the adjacency circle located at the extreme left and at the extreme right of the room (Fig. 31). Finally, the general flowchart for the recognition of the different entities is given in Fig. 33.

4 Conclusion

Based on the hybrid graphs/rules AMFR approach, we propose in this paper a novel compliant CAPP-STEP-NC system for machining rotational parts. The AMFR firstly decodes the basic geometrical and topological entities

from the part's ISO AP203 CAD STEP file and reconstitutes them as machining features by applying established rules which are stored in the internal library of the system. Secondly, these detected features are converted into normalized entities according to the ISO 14649 standard. After defining the manufacturing parameters, the machining strategies and the cutting tools, and their mapping to the attributes of the classes of the same ISO standard 14,649, the writing of the final STEP-NC file for machining the part is generated.

This AMFR algorithm, powered and structured using tree modeling, is capable of the following:

1. Recognizing and differentiating between external and internal features by giving their graph/tree replacing the classic method of individual feature recognition
2. Identifying frontal and axial features for each external and internal identified graph-tree
3. Selecting interacting features from simple features and allowing suitable treatments to give alternative sequencing to ensure their machining.






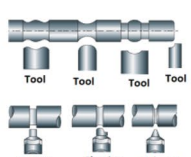





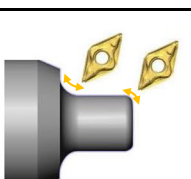


The AMFR algorithm was developed and validated using a practical case of a turning part containing diverse features: external/internal, simple/interacting and axial/frontal.

The purpose of this work was to implement the new standard STEP-NC in a CAPP turning process and remedy the shortcomings of ISO 6893 G-code to overcome modern manufacturing demands. To that end, a new consistent-fast algorithm that allows the extraction of a part's machining turning entities with improved efficiency and complex geometry was elaborated. Further, this work introduced the main machining entities defined within the framework of this standard and explained the different parameters necessary for unambiguous definition of these entities whether of a geometric, topological or other nature.

As mentioned, the AMFR of the elaborated CAPP-Turn is based on a smart algorithm that can handle the common turning features, thus ensuring machining of rotational parts with complex geometry. In addition, the algorithm includes detection and treatment of the frontal turning features, because we believe that these features have not received sufficient attention by researchers despite their functional aspects in mechanical systems that justify their presence in numerous designed parts (labyrinth seals, seal positioning, thrust bearing, etc.).

Appendix 1

Table 5 A The exported STEP-NC programs (partial) for machining the assembly interfaces

Cylindrical turning		Symetry axis of turning part ----- movement of the tool with regard to the axis of revolution	Facing circular groove		Symetry axis of turning part ----- movement of the tool with regard to the axis of revolution
Facing turning		Symetry axis of turning part ----- movement of the tool with regard to the axis of revolution	Thread		Symetry axis of turning part ----- movement of the tool with regard to the axis of revolution
Axial shoulder		Symetry axis of turning part ----- movement of the tool with regard to the axis of revolution	Shape turning		Symetry axis of turning part ----- movement of the tool with regard to the axis of revolution
Conical turning		Symetry axis of turning part ----- movement of the tool with regard to the axis of revolution	cutoff side		Symetry axis of turning part ----- movement of the tool with regard to the axis of revolution
Profiling		Symetry axis of turning part ----- movement of the tool with regard to the axis of revolution	chamfering		Symetry axis of turning part ----- movement of the tool with regard to the axis of revolution
Radial circular groove		Symetry axis of turning part ----- movement of the tool with regard to the axis of revolution	corner rounding		Symetry axis of turning part ----- movement of the tool with regard to the axis of revolution
Radial recess		Symetry axis of turning part ----- movement of the tool with regard to the axis of revolution	Knurling		Symetry axis of turning part ----- movement of the tool with regard to the axis of revolution

Appendix 2

Table 6 A The exported STEP-NC programs (partial) for machining the assembly interfaces

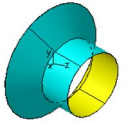
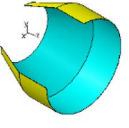
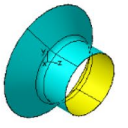
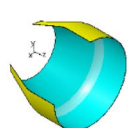
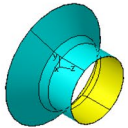
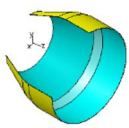
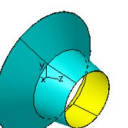
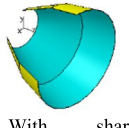
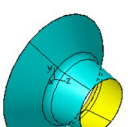
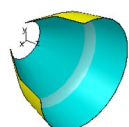
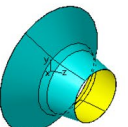
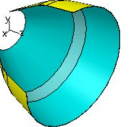
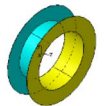

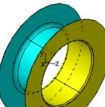

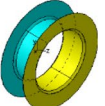

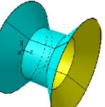
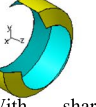
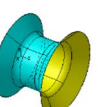

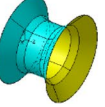

Name of entity	Exterior Compound Entity	Inner Compound Entity	Entity recognition rules
Inclined shoulder type I	 <p>With sharp circular edge</p>	 <p>With sharp circular edge</p>	<ol style="list-style-type: none"> Existence of a basic Entity of cylinder type defined above Existence of a cone delimited by two circular loops Loop1 and Loop2 defined on the screen. The Cylinder must share its inner Loop (small diameter) with the Cone. The angle between the surface of the cone and the surface of the cylinder must be between 90° and 180°.
	 <p>With fillet</p>	 <p>With fillet</p>	<ol style="list-style-type: none"> Existence of a basic Entity of cylinder type defined above. Existence of a cone delimited by two concentric circular loops Loop1 and Loop2 defined on the screen. Existence of a fillet delimited by two circular loops defined on the screen. The fillet must share with the Cylinder its small diameter Loop and with the cone its large diameter Loop. The Toroidal surface Tor1 of the fillet must be tangent to the Cylinder and to the cone: the ArcCirc11 dividing the two toroidal surfaces must be tangent to the line Line21 dividing the two cylindrical surfaces and to the dividing line of the two conical surfaces. The angle between the surface of the cone and the surface of the cylinder must be between 90° and 180°.
	 <p>With chamfer</p>	 <p>With chamfer</p>	<ol style="list-style-type: none"> Existence of a basic Entity of cylinder type defined above Existence of two cones each delimited by two circular loops defined in the screen. The cone (thin thickness) must share its small diameter Loop with the Cylinder and its large diameter Loop with the cone. The angle between the surface of the cone and the surface of the cylinder must be between 90° and 180°.
Epaulement Incliné type II	 <p>With sharp circular edge</p>	 <p>With sharp circular edge</p>	<ol style="list-style-type: none"> Existence of two cones defined on the screen, each delimited by two circular loops. The two cones must share a Circular Loop. The angle between the two cones should be between 90° and 180°.
	 <p>With fillet</p>	 <p>With fillet</p>	<ol style="list-style-type: none"> Existence of two cones Cône1 and Cône2 defined with screens each delimited by two circular loops. Existence of a fillet defined on the screen delimited by two circular loops. The fillet must share its small diameter Loop with one of the two cones and its large diameter Loop with the other cone. The Toroidal surface Tor1 of the fillet must be tangent to the two cones: the ArcCirc11 dividing the two toroidal surfaces must be tangent to the dividing line Line12 of the two conical surfaces of cone1 and to the dividing line Line21 of the two conical surfaces of cone2
	 <p>With chamfer</p>	 <p>With chamfer</p>	<ol style="list-style-type: none"> Existence of three cones Cone1 and Cone2 and cone 3 defined with screens each delimited by two circular loops. One of the three cones (low thickness) must share with one of the other two cones its small diameter loop and with the remaining cone its large diameter loop.

Table 6 (continued)

Name of entity	Exterior Compound Entity	Inner Compound Entity	Entity recognition rules
Normal groove	 With sharp circular edge	 With sharp circular edge	<ol style="list-style-type: none"> Existence of a basic Entity of cylinder type defined above Existence of two Plans Type2 Plan1 and Plan2 defined previously: each delimited by two concentric circular loops. Let (Loop11 and Loop12) for Pan1 and (Loop21 and Loop22) for Plan2. The Cylinder must share with Plan1 the inner loop of the couple (Loop11 and Loop12) and with Plan 2 the inner Loop of the couple (Loop21 and Loop22) °.
	 With fillet	 With fillet	<ol style="list-style-type: none"> Existence of a basic Entity of cylinder type defined above Existence of two Plans Type2 Plan1 and Plan2 defined on the screen: each delimited by two concentric circular loops. Let (Loop11 and Loop12) for Pan1 and (Loop21 and Loop22) for Plan2. Existence of two separate leaves each delimited by two circular loops defined on the screen. Let (Boucle11 and Boucle12) for Fillet1 and (Boucle21 and Boucle22) for Fillet2 Fillet1 must share with Cylinder and Plane1 or Plane2 the Small Diameter Loop and the Large Diameter Loop respectively. If Fillet1 and Plane1 share the same loop Then Fillet2 must share with Plan2 the large diameter Loop of the couple (Boucle21 and Boucle22) if not Fillet2 must share with Plan1 the large diameter loop of the couple (Boucle11 and Boucle12) The Toroidal surface of each fillet must be tangent to the Cylinder and plane surfaces adjacent to it
	 With chamfer	 With chamfer	<ol style="list-style-type: none"> Existence of a basic Entity of cylinder type defined above Existence of two cones each delimited by two circular loops defined in the screen. The cone (thin thickness) must share its small diameter Loop with the Cylinder and its large diameter Loop with the cone. The angle between the surface of the cone and the surface of the cylinder must be between 90° and 180°.
Inclined groove	 With sharp circular edge	 With sharp circular edge	<ol style="list-style-type: none"> Existence of two cones defined on the screen, each delimited by two circular loops. The two cones must share a Circular Loop. The angle between the two cones should be between 90° and 180°.
	 With fillet	 With fillet	<ol style="list-style-type: none"> Existence of two cones Cône1 and Cône2 defined with screens each delimited by two circular loops. Existence of a fillet defined on the screen delimited by two circular loops. The fillet must share its small diameter Loop with one of the two cones and its large diameter Loop with the other cone. The Toroidal surface Tor1 of the fillet must be tangent to the two cones: the ArcCirc11 dividing the two toroidal surfaces must be tangent to the dividing line Line12 of the two conical surfaces of cone1 and to the dividing line Line21 of the two conical surfaces of cone2
	 With chamfer	 With chamfer	<ol style="list-style-type: none"> Existence of three cones Cone1 and Cone2 and cone 3 defined with screens each delimited by two circular loops. One of the three cones (low thickness) must share with one of the other two cones its small diameter loop and with the remaining cone its large diameter loop.

Appendix 3: A The exported STEP-NC programs (partial) for machining the assembly interfaces

Mathematical definition of B-spline function

The B-spline function with non-uniform nodes is defined by

$$B(t) = \sum_{i=0}^n b_i(t) \cdot N_{i,d}(t) \quad t_i \leq t < t_{i+1} \quad (1)$$

where: the $b_i(t)$ are the control points, and the $N_{i,d}(t)$ are the basis functions of degree d (dgrebspline) given by the following Deboor–Cox recurrence relation:

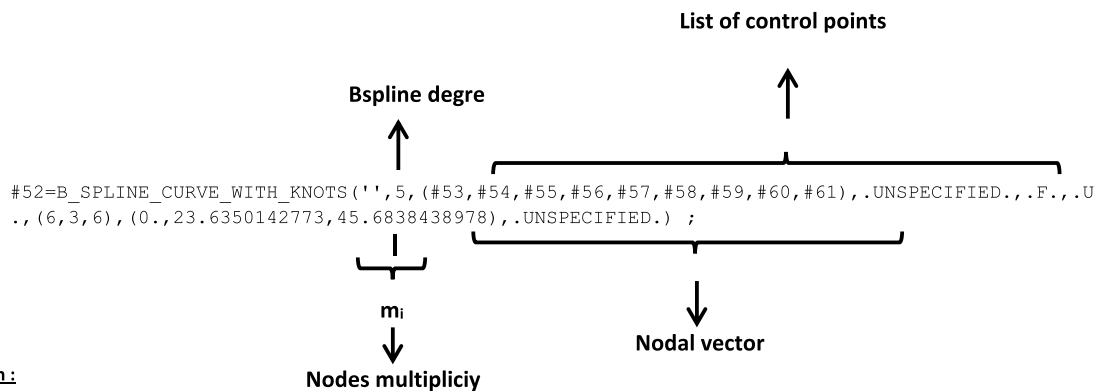
$$N_{i,0}(t) = \begin{cases} 1 & \text{if } t_i \leq t < t_{i+1} \\ 0 & \text{si non} \end{cases} \quad (2)$$

and

$$N_{i,d}(t) = \frac{(t - t_i)N_{i,d-1}(t)}{t_{i+d} - t_i} + \frac{(t_{i+d+1} - t)N_{i+1,d-1}(t)}{t_{i+d+1} - t_{i+1}} \quad (3)$$

Data provided by the STEP file

The parameters provided by the STEP format, allowing the definition of the B-spline function, are summarized by the diagram in the following figure:



With :

#53, #54, #55, #56, #57, #58, #59, #60, #61 sont les points cartésiens définissant le points de contrôle **Pi (t)** et sont donnés par :

```
#53=CARTESIAN_POINT('Control Point', (0., 32.0395202637, 0.)) ;
#54=CARTESIAN_POINT('Control Point', (0., 36.6456050288, 1.6526988121)) ;
#55=CARTESIAN_POINT('Control Point', (0., 41.0291359978, 3.60052324714)) ;
#56=CARTESIAN_POINT('Control Point', (0., 45.1901131706, 5.84347330512)) ;
#57=CARTESIAN_POINT('Control Point', (0., 52.8026458577, 10.7492902362)) ;
#58=CARTESIAN_POINT('Control Point', (0., 59.5837047882, 16.7577134342)) ;
#59=CARTESIAN_POINT('Control Point', (0., 62.662827713, 19.9144582004)) ;
#60=CARTESIAN_POINT('Control Point', (0., 65.5482663676, 23.3280450961)) ;
#61=CARTESIAN_POINT('Control Point', (0., 68.240020752, 26.9984741211)) ;
```

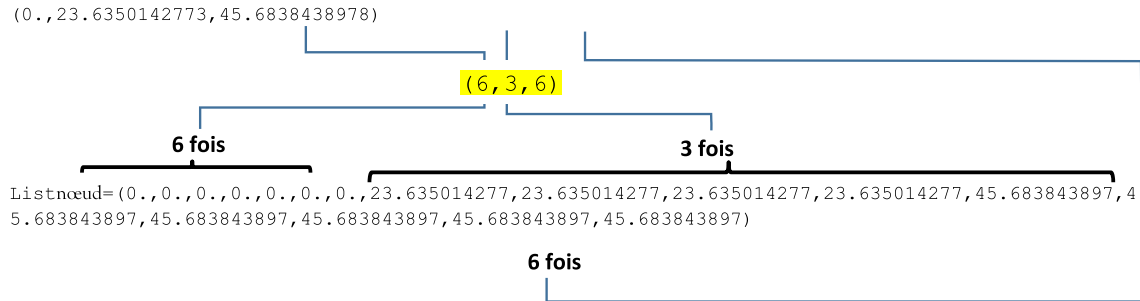
The summation parameter n is given by:

$$n = m - \text{degreespline} - 1$$

m is the sum of multiplicity of each nodes: $m = \sum_{i=1}^m m_i$

etd and the B-spline degree denoted by degreespline is given directly by the STEP file.

Using the information provided by STEP we build the list of nodes from the nodal vector by cloning in order m_i times each node i of the nodal vector:



The list of control points $bi(t)$ is defined in the plane and it is given by eliminating the zero of each control point $P_i: bi(t) = [(32.0395202637, 0.), (36.6456050288, 1.6526988121), (41.0291359978, 3.60052324714), (45.1901131706, 5.84347330512), (52.8026458577, 10.7492902362), (59.5837047882, 16.7577134342), (62.662827713, 19.9144582004), (65.5482663676, 23.3280450961), (68.240020752, 26.9984741211)]$.

Algorithm for calculating the ordinate (radius of the section) f(Z) at Z defined for a B-spline profile:

Entrance :

o The degree of the B-spline: Listnœud=(0., 0., 0., 0., 0., 0., 0., 0., 23.635014277, 23.635014277, 23.635014277, 23.635014277, 45.683843897, 45.683843897, 45.683843897, 45.683843897, 45.683843897, 45.683843897) .

o List of nodes:

Listnœud=(0., 0., 0., 0., 0., 0., 0., 0., 23.635014277, 23.635014277, 23.635014277, 23.635014277, 45.683843897, 45.683843897, 45.683843897, 45.683843897, 45.683843897, 45.683843897) .

o List of control points: $bi(t) = [(32.0395202637, 0.), (36.6456050288, 1.6526988121), (41.0291359978, 3.60052324714), (45.1901131706, 5.84347330512), (52.8026458577, 10.7492902362), (59.5837047882, 16.7577134342), (62.662827713, 19.9144582004), (65.5482663676, 23.3280450961), (68.240020752, 26.9984741211)]$.

Processing :

o Determination of the basis functions of the B-spline $N[i, \text{degreespline}]$ as a function of $N[i, 0]$ for going from 1 to n using the established and tested algorithm given by the next page

o Determination of the B-spline function using the following algorithm:

B-spline=0;

Pouri ranging from 0 to degreespline

To do

 B-spline: B-spline + b(j).N[j, degreespline]

End Do

o Determination of the B-spline function for each interval of the parameter t defined from the nodal vector using the condition:

$$N[i, 0] = \begin{cases} 1 & \text{si } t_i < t < t_{i+1} \\ 0 & \text{Ailleurs} \end{cases}$$

Each interval corresponds to the couple $(Z=f(t),f(Z)=g(t))$.

For d ranging from 1 to degreespline`

```

Faire
  Pouri allant de 0 jusqu'à n
  Faire
    Si t[i+d]=t[i] et t[i+d+1]≠t[i+1] alors
      N[i, d] =  $\frac{t[i+d+1]-t}{t[i+d+1]-t[i+1]}$ . N[i + 1, d - 1] Si non
      Si t[i+d+1]=t[i+1+1] et t[i+d] ≠t[i+1] alors
        N[i, d] =  $\frac{t-t[i]}{t[i+d]-t[i]}$ . N[i, d - 1] Si non
        Si t[i+d]=t[i] et t[i+d+1]=t[i+1] alors
          N[i,d]=0. si non
          N[i, d] =  $\frac{t-t[i]}{t[i+d]-t[i]}$ . N[i, d - 1] +  $\frac{t[i+d+1]-t}{t[i+d+1]-t[i+1]}$ . N[i + 1, d - 1]
        fin Si
      fin Si
    fin Si ;
  A[i,d]= N[i,d]
Fin Faire ;
Pouri allant de 0 jusqu'à n
Faire
  N[i,d-1]:=A[i,d-1];
Fin Faire;
Pouri allant de 0 jusqu'à n
Faire
  Si t[i+d]=t[i] et t[i+d+1]≠t[i+1] alors
    x[i,d]:=  $\frac{t[i+d+1]-t}{t[i+d+1]-t[i+1]}$ . N[i + 1, d - 1] Si non
  Si t[i+d+1]=t[i+1] et t[i+d]>=t[i] alors
    x[i,d]:= N[i, d] =  $\frac{t-t[i]}{t[i+d]-t[i]}$ . N[i, d - 1] Si non
    Si t[i+d]=t[i] et t[i+d+1]=t[i+1] alors
      x[i,d]=0. Si non
      x[i,d]=  $\frac{t-t[i]}{t[i+d]-t[i]}$ . N[i, d - 1] +  $\frac{t[i+d+1]-t}{t[i+d+1]-t[i+1]}$ . N[i + 1, d - 1]
    fin Si
  fin Si
Fin Si;
Fin Faire
  
```

Authors' contributions Methodology, investigation, writing original draft preparation and visualization: EL Mesbahi Abdelilah. Supervision: Irene-buj Corral and EL Mesbahi Jihad. Conceptualization: Bensaid Oussama.

Data availability All the data and material are available upon request to the corresponding author.

Code availability Code sharing is not applicable to this article as no new code was created in this study.

Declarations

Competing interest The authors declare that they no known competing financial interests or personal relationships that could have appeared to influence the work reported in this paper.

Ethical approval The article involves no studies on human or animal subjects.

Consent to participate Not applicable.

Consent to publish The publisher has the permission of the authors to publish the given article.

References

- Sivakumar S, Dhanalakshmi V (2013) A feature-based system for CAD/CAM integration through STEP file for cylindrical parts. Indian J Eng Mater Sci 20(February):21–26
- Malleswari VN, Valli PM, Sarcar MMM (2013) Automatic Recognition of Machining Features using STEP Files. Int J Eng Res Technol (IJERT) 2(3) ISSN: 2278–0181
- TAHİR FİDAN (2004) Automatic Recognition of Machining Features using STEP Files, thesis submitted to the graduate school of natural and applied sciences of Middle East Technical University METU Turkey.
- Sharma R, Gao JX (2002) Implementation of STEP 224 in an Automated Manufacturing Planning System. Proc Inst Mech Eng B Eng 216(9):1277–1289
- Xu XW (2006) Realization of STEP-NC enabled machining. Robot Comput-Integr Manuf 22(2):144–53
- Suh SH, Chung DH, Lee BE, Shin S, Choi I, Kim KM (2006) STEP-compliant CNC system for turning: data model, architecture, and implementation. Comput Aided Des 38(6):677–88
- Xu WX, Liu Y, Zhao GY, Zheng DB (2006) Study on conversion from STEP-NC into G-code. In the International Symposium on Advances in Abrasive Technology, Dalian, Peoplesr China, pp.566–571
- Shin SJ, Suh SH, Stroud I (2007) Reincarnation of G-code based part programs into STEP-NC for turning applications. Comput Aided Des 39(1):1–16
- Suh SH, Lee BE (2004) STEP-manufacturing roadmap. In: Proceedings of Korea CAD/CAM conference, Kangwon, Korea
- Zhang X, Liu R, Nassehi A, Newman ST (2011) A STEP-Compliant process planning system for CNC turning operations. Robot Comput-Integr Manuf 27:349–356
- Yusof Yusri, Case Keith (2008) STEP Compliant CAD/CAPP/CAM System for Turning Operations, Proceedings of the World Congress on Engineering and Computer Science 2008 WCECS 2008, October 22 - 24, San Francisco, USA
- Čuboňová N (2013) Creation of software for the transformation of Step-Nc Data. Acad J Manuf Eng 11(4/2013)
- Suh Suk-Hwan et al (2006) STEP-compliant CNC system for turning: Data model, architecture and implementation. Comput-Aided Des 38:677–688
- Xu XW, Wang H, Mao J, Newman ST, Kramer TR, Proctor FM, JL (2005) Michaloski. STEP-compliant NC research: the search for intelligent CAD/CAPP/CAM/CNC integration. Int J Prod Res 43(17):1 3703–3743

15. Hardwick M (2010) Third-generation STEP systems that aggregate data for machining and other applications. *Int J Comput Integr Manuf* 23:893–904
16. Newman ST, Nassehi A, Xu XW, Rosso RSU Jr, Wang L, Yusof Y, Ali L, Liu R, Zheng LY (2008) Strategic advantages of interoperability for global manufacturing using CNC technology. *Robot Comput-Integr Manuf* 24:699–708
17. Girnth Simon, Koopmann Julian, Klawitter Günter, Waldt Nils, Niendorf Thomas (n.d.) 3D hybrid-material processing in selective laser melting: implementation of a selective coating system. *Prog Addit Manuf*. <https://doi.org/10.1007/s40964-019-00082-w>
18. Bhushan Bharat, Caspers Matt (n.d.) An overview of additive manufacturing (3D printing) for microfabrication, *Microsyst Technol*. <https://doi.org/10.1007/s00542-017-3342-8>.
19. Chen Michael Y, Skewes Jacob, Woodruff Maria A, Dasgupta Prokar, Rukin Nicholas J (2020) Multi-colour extrusion fused deposition modelling: a low-cost 3D printing method for anatomical prostate cancer models. *Sci Rep*. <https://doi.org/10.1038/s41598-020-67082-7>
20. Haghbin N, Bone D, Young K (2021) Controlled extrusion-based 3D printing of micro-channels with the geometric modelling of deposited roads. *J Manuf Process* 67:406–417. <https://doi.org/10.1016/j.jmapro.2021.04.067>
21. Zhao Donghua, Guo WZ (2018) Research on Curved Layer Fused Deposition Modeling (CLFDM) With Variable Extruded Filament (VEF), Conference Paper. <https://doi.org/10.1115/DETC2018-85343>
22. Jin Yu-an, Li Hui, He Yong, Fu Jian-zhong (2015) Quantitative analysis of surface profile in fused deposition modelling. *Addit Manuf*. <https://doi.org/10.1016/j.addma.2015.10.001>.
23. Martini M, Scaccia M, Marchello G, Abidi H, D'Imperio M, Cannella F (2022) An Outline of Fused Deposition Modeling: System Models and Control Strategies. *Appl Sci* 12:5400. <https://doi.org/10.3390/app12115400>
24. Vicente Carlos MS, Martins Tomás S, Leite Marco, Ribeiro António, Reis Luís (n.d.) Influence of fused deposition modeling parameters on the mechanical properties of ABS parts. *Polym Adv Technol Pat* 4787. <https://doi.org/10.1002/pat.4787>
25. Tomás Sousa Martins (n.d.) Study of the Processing Parameters Influence on the Mechanical Properties of ABS parts fabricated by FDM. https://fenix.tecnico.ulisboa.pt/downloadFile/281870113704291/Extended-Abstract_72938.pdf.
26. Hussein HMA, Abou Oual Nasr Emad, Khan Awis (2013) Automated feature extraction from cylindrical parts based on STEP, International Conference on Sustainable Intelligent Manufacturing (SIM 2013), Lisbon, Portugal, 26–29
27. Qin Guofeng, Li Qiyang (2005) Study of the Intelligent Turning Machining Method Based on Geometrical Feature Recognition, pp. 261–270, Cooperative Design, Visualization, and Engineering, Second International Conference by Yuhua Luo, CDVE 2005 Palma de Mallorca, Spain, September 18–21, Proceedings
28. Chung C, Peng Q (2013) Data Representation and Modeling for Process Planning, Semantic Modeling and Interoperability in Product and Process Engineering, Y.-S. Ma Editor, Springer Series in Advanced Manufacturing
29. Ketan Hussein Salem (2010) Built automatic feature recognition system based on sweeping primitive, The Seventh Jordanian International Mechanical Engineering Conference.
30. Yildiz Yakup, Korkut İhsan, Şeker Ulvi, GU (2006) Development of a Feature Based CAM System for Rotational Parts. *J Sci* 19(1):35–40
31. El Mesbahi Abdelilah (2009) A new methodology for recognition of interacting features using Frontier Faces of Base Face, sixième Conférence Internationale de Conception et Production Intégrées, CPI 2009 Organisée à Fès 19–21 Octobre 2009
32. El Mesbahi Abdelilah, Jaider Oussama, Rechia Ahmed (2014) Automatic Recognition of Isolated And Interacting Manufacturing Features In : Milling Process, *Int. Journal of Engineering Research and Applications*, Vol. 4, Issue 10 (Part - 2), pp.57–72
33. Reddy Sreekar et al. (2016) An Intelligent feature based process planning for Rotational parts, Proceedings of the 2016 International Conference on Industrial Engineering and Operations Management Kuala Lumpur, Malaysia, March 8–10, 2016
34. Safaieh Mehrdad, Nassehi Aydin, Newman Stephen T (2013) A novel methodology for cross-technology interoperability in CNC machining. *Robot Comput-Integr Manuf* 29(3):79–87
35. El Hakim Mohamed A, Afifi Atef A, Elmesallamy Ahmed S (2009) Computer aided process planning of turned parts. *Eng Res J* 122:m26-m38
36. Zhao Y, Ridgway Keith, Al-Ahmari AMA (2002) Integration of CAD and a cutting tool selection system. *Comput Ind Eng* 42:17–34
37. Madurai Srinivasakumar S, Lrn Li (1992) Rule-based Automatic Part Feature Extraction and Recognition from CAD DATA. *Comput Ind Eng* 22(1):49-62
38. Seeram Srinivasa Rao, Ali Md Abid, Karimulla Syed (2016) Automatic Recognition of Internal Features of Axisymmetric Parts from 2-D Images. *Indian J Sci Technol* 9(44)
39. Muljadi H, Ando K, Takeda H (2005) Considering Designer's Intention for the Extraction of Manufacturing Feature, 18th International Conference on Production Research.
40. Simple, multi-material 3D printing, Palette 2, <https://www.mosai cmfg.com>. Accessed 28 July 2022.
41. Shanmugam R, Vinayagam M, Ramoni MO, Lakshmanan P (2021) A Review on the significant classification of Additive Manufacturing. *J Phys Conf Ser*. <https://doi.org/10.1088/1742-6596/2027/1/012026>.
42. Dizon John Ryan C, Espera Jr Alejandro H, Chen Qiyi, Rigoberto C (2018) Advinculaa, Mechanical characterization of 3D-printed polymers. *Additive Manufacturing* 20:44–67. <https://doi.org/10.1016/j.addma.2017.12.002>
43. Chakraborty Samit, Biswas Manik Chandra (2020) 3D printing technology of polymer-fiber composites in textile and fashion industry: A potential roadmap of concept to consumer. *Compos Struct* 248:112562. <https://doi.org/10.1016/j.compstruct.2020.112562>
44. Shahrubudin N, Lee TC, Ramlan R (2019) An Overview on 3D Printing Technology: Technological, Materials and Applications. *Procedia Manuf* 35:1286–1296. <https://doi.org/10.1016/j.promfg.2019.06.089>
45. SherDavide (2022) Mcor's new arke 3d printer ushers in full-color desktop 3d printing for all <https://3dprintingindustry.com/news/64028-64028>, Accessed 09 September 2022
46. Stichel Thomas, Laumer Tobias, Wittmann Peter, Amend Philipp, Roth Stephan (2015) Selective deposition of polymer powder by vibrating nozzles for laser beam melting, Lasers in Manufacturing Conference.
47. Liu Baoqing, Xu Zilong, Fan Fangyi, Huang Bolin (2018) Experimental study on the solid suspension characteristics of coaxial mixers. *Chem Eng Res Des* 133:335–346. <https://doi.org/10.1016/j.cherd.2018.03.035>
48. Ghanem Akram, Lemenand Thierry, Della Valle Dominique, Peerhossaini Hassan (2014) Static mixers: Mechanisms, applications, and characterization methods – A review. *Chem Eng Res Des* 92:205–228. <https://doi.org/10.1016/j.cherd.2013.07.013>
49. Gikanga B, Maa Y-F (2020) A Review on Mixing-Induced Protein Particle Formation: The Puzzle of Bottom-Mounted Mixers. *J Pharm Sci* 109:2363–2374. <https://doi.org/10.1016/j.xphs.2020.03.024>
50. Musiał M, Cudak M, Karcz J (2017) Numerical analysis of momentum transfer processes in a mechanically agitated air

- biophase – liquid system. *Chem Process Eng* 38(3):465–475. <https://doi.org/10.1515/cpe-2017-0036>
51. Kumar Ashok (n.d.) Design and Fabrication of Bottom Pouring Type Stir Casting Furnace with Carrier Gas, <https://www.researchgate.net/publication/339103679>.
 52. Wilczyński Krzysztof, Nastaj Andrzej, Lewandowski Adrian, Wilczyński Krzysztof J, Buziak Kamila (2019) Fundamentals of Global Modeling for Polymer Extrusion. *Polymers* 11:2106. <https://doi.org/10.3390/polym11122106>
 53. Dhaval Mori, Sharma Shweta, Dudhat Kiran, Chavda Jayant (n.d.) Twin-Screw Extruder in Pharmaceutical Industry: History, Working Principle, Applications, and Marketed Products: an In-depth Review. *J Pharm Innov.* <https://doi.org/10.1007/s12247-020-09520-7>
 54. CPM Extricom Extrusion (n.d.) High Capacity Multi Screw Extruder for Linoleum Mixing and Pharmaceutical Compounding, <http://www.cpmruiaextrusion.com/sale-11043870-high-capacity-multi-screw-extruder-for-linoleum-mixing-and-pharmaceutical-compounding.html>
 55. CAPSULCN (n.d.) V Blender Dry Powder Mixer Blending Machine V50 - V300, <https://www.ipharmachine.com/high-capacity-v-blender-dry-powder-mixer-blending-machine>
 56. MAZERUSTAR (n.d.) Planetary mixer, <https://www.kurabo.co.jp/bio/English/mazerustar>
 57. Bhoite Kiran, Kakandikar GM, Nandedkar VM (2015) Schatz Mechanism with 3D-Motion Mixer-A Review, 4th International Conference on Materials Processing and Characterization. *Mater Today Proc* 2:1700–1706. <https://doi.org/10.1016/j.matpr.2015.07.003>
 58. Hirschberg S, Koubek R, Moser F, Schöckb J (2009) An improvement of the Sulzer SMXTM static mixer significantly reducing the pressure drop. *Chem Eng Res Des* 87:524–532. <https://doi.org/10.1016/j.cherd.2008.12.021>
 59. Coroneo Mirella, Montante Giuseppina, Paglianti Alessandro (n.d.) Computational Fluid Dynamics Modeling of Corrugated Static Mixers for Turbulent Applications. *Ind Eng Chem Res.* <https://doi.org/10.1021/ie300398z>
 60. Lobry Emeline, Theron Félicie, Gourdon Christophe, Le Sauze Nathalie, Xuereb Catherine, Lasuye Thierry (2011) Turbulent liquid–liquid dispersion in SMV static mixer at high dispersed phase concentration. *Chem Eng Sci* 66:5762–5774. <https://doi.org/10.1016/j.ces.2011.06.073>
 61. Primit Performance by Design (2017) Mixing and conditioning of liquids and gases, static mixers & heat exchangers. *Chem Process Eng* 38(3):465–475. https://www.raimaberfluidtech.com/wp-content/uploads/2021/06/company_brochure.pdf
 62. Hsu C-W, Shih P-T, Chen JM (2020) Enhancement of Fluid Mixing with U-Shaped Channels on a Rotating Disc. *Micromachines* 11:1110. <https://doi.org/10.3390/mi11121110>
 63. IDEX Health & Science, PEEK Manifold Assembly 9 Port, for 1/8" OD, <https://www.idex-hs.com/store/fluidics/fluidic-connections/connectors/low-pressure-multiport-connectors/peek-manifold-assembly-9-port-for-1-8-od.html>
 64. Tao Jinsong et al. (2019) Application of flash nanoprecipitation to fabricate poorly water-soluble drug nanoparticles. *Acta Pharm Sin B* 9(1):4–18. <https://doi.org/10.1016/j.apsb.2018.11.001>
 65. Kuo HP, Knight TPC, Parkerc DJ, Seville JPK (2005) Solids circulation and axial dispersion of cohesionless Particles in a V-mixer. *Powder Technol* 152:133–140. <https://doi.org/10.1016/j.powtec.2004.12.003>
 66. CoroBore 824EH - SC, Ø1 – 8.2 mm, CoroBore 824 XS, New boring concepts, Sandvik Coromant, <https://www.sandvik.coromant.com/en-gb/products/corobore-824-xs/pages/default.aspx>
 67. Da vinci color printer 3D; [https://www.xyzprinting.com/en-](https://www.xyzprinting.com/en-68)
 68. US/product-level/PROFESSIONAL/color-series.

Publisher's note Springer Nature remains neutral with regard to jurisdictional claims in published maps and institutional affiliations.

Springer Nature or its licensor (e.g. a society or other partner) holds exclusive rights to this article under a publishing agreement with the author(s) or other rightsholder(s); author self-archiving of the accepted manuscript version of this article is solely governed by the terms of such publishing agreement and applicable law.